Interactome Mapping Guided by Tissue-Specific Phosphorylation in Age-Related Macular Degeneration

Srinivas R. Sripathi,[1,2] Weilue He,[3] Cameron L. Prigge,[1,4] O'Donnell Sylvester,[5] Ji-Yeon Um,[1,6] Folami L. Powell,[7] Musa Neksumi,[8] Paul S. Bernstein,[9] Dong-Won Choo,[10] Manuela Bartoli,[7] Diana R. Gutsaeva,[7]* and Wan Jin Jahng[5]*

Abstract— The current study aims to determine the molecular mechanisms of age-related macular degeneration (AMD) using the phosphorylation network. Specifically, we examined novel biomarkers of oxidative stress by protein interaction mapping using *in vitro* and *in vivo* models that mimic the complex and progressive characteristics of AMD. We hypothesized that the early apoptotic reactions could be initiated by protein phosphorylation in region-dependent (peripheral retina vs. macular) and tissue-dependent (retinal pigment epithelium vs. retina) manner under chronic oxidative stress. The analysis of protein interactome and oxidative biomarkers showed the presence of tissue- and region-specific post-translational mechanisms that contribute to AMD progression and suggested new therapeutic targets that include ubiquitin, erythropoietin, vitronectin, MMP2, crystalline, nitric oxide, and prohibitin. Phosphorylation of specific target proteins in RPE cells is a central regulatory mechanism as a survival tool under chronic oxidative imbalance. The current interactome map demonstrates a positive correlation between oxidative stress-mediated phosphorylation and AMD progression and provides a basis for understanding oxidative stress-induced cytoskeletal changes and the mechanism of aggregate formation induced by protein phosphorylation. This information could provide an effective therapeutic approach to treat age-related neurodegeneration.

Index Terms— age-related macular degeneration, mitochondria, oxidative stress, prohibitin, protein interactome, proteomics, retinal pigment epithelium

1 INTRODUCTION

IN an oxidative environment, eukaryotic cells exhibit central signaling responses including ATP-mediated reversible protein phosphorylation at serine, threonine, or tyrosine residues [1,2]. These transient post-translational modifications in response to extracellular and mitochondrial stressors control apoptosis of retinal pigment epithelial (RPE) cells within a very short timeframe. The RPE is a supportive layer of cells that are essential for the health of rod and cone photoreceptors [2]. Progressive cell death of post-mitotic RPE can lead to age-related macular degeneration (AMD), which results from rod and cone apoptosis. RPE cells are exposed to chronic oxidative stress, including constant exposure to intense light and reactive oxygen species (ROS) from mitochondria due to high levels of oxygen consumption. However, the mechanisms of oxidative stress-mediated phosphoproteomic alterations that initiate death signals in the RPE remain elusive. Further, details regarding phosphorylation signaling in AMD are complicated due to the dynamics of phosphorylation reactions lasting from seconds to minutes, as compared to the slow kinetics of the aging process, which occurs over years in the retina.

Proteomic approaches that include 2D gel electrophoresis and protein identification by mass spectrometry have been used routinely for the last decade to study protein identification and modifications. However, RPE phosphoproteomics in AMD remains challenging due to the complex metabolism and sub-stoichiometry of phosphoproteins. For this reason, proteomic studies using *in vivo* models that mimic the complex and progressive characteristics of AMD are extremely valuable for studying the pathogenesis of AMD and testing different treatment modalities [3–6].

Unbiased proteomic approaches demonstrated that the early apoptotic network and post-translational mechanisms exist to determine RPE cell survival or death under stress conditions.

• *Wan Jin Jahng, Retina Proteomics Laboratory and Organic Chemistry Laboratory, Department of Petroleum Chemistry, American University of Nigeria, Yola, Nigeria, PH +234 805 550 1032. E-mail: wan.jahng@aun.edu.ng
• *Diana R. Gutsaeva, Department of Ophthalmology, Augusta University, Augusta, GA, USA, PH +1 706 721 7910. E-mail: dgutsaeva@augusta.edu
[1] Department of Biological Sciences, Michigan Technological University, Houghton, MI, USA
[2]Department of Ophthalmology, Wilmer Eye Institute, The Johns Hopkins University School of Medicine, Baltimore, MD, USA
[3]Department of Biomedical Engineering, Michigan Technological University, Houghton, MI, USA
[4]Department of Neurobiology, Duke University, North Carolina, USA
[5]Department of Petroleum Chemistry, American University of Nigeria, Yola, Adamawa, Nigeria
[6]Department of Optometry, Seoul National University of Science and Technology, Seoul, Korea
[7]Department of Ophthalmology, Augusta University, Augusta, GA, USA
[8]Department of Chemistry, Modibbo Adama University of Science and Technology, Yola, Adamawa, Nigeria
[9]Department of Ophthalmology and Visual Sciences, Moran Eye Center, University of Utah School of Medicine, Salt Lake City, UT, USA
[10]Department of Bioinformatics, Korea Polytechnic University, Geonggi, Korea

International Journal of Scientific & Engineering Research, Volume 8, Issue 2, February -2017
ISSN 2229-5518

Early signaling molecules under oxidative stress, including erythropoietin (EPO), crystallins, vimentin, protein phosphatase 2A (PP2A), hypoxia inducible factor-1 (HIF1), JAK2, prohibitin, RPE65, and nitric oxide synthase (NOS), are modulated and hyperphosphorylated *in vitro* and *in vivo* [7–9]. For instance, phosphorylations of crystallin and vimentin may participate in the pathogenesis of AMD by forming soft drusen with longer chain phosphatidylcholine and cholesteryl esters [10,11].

In the current study, we seek to determine whether tightly regulated phosphorylation reactions in RPE cells are critical to maintain cytoskeletal integrity and cell survival under chronic oxidative stress. Our objective is to examine the molecular network of altered phosphorylation to determine initial targets to treat AMD in the early stage. We examined a novel role of phosphorylated biomarkers as an adaptation to extracellular stress and used the phosphoproteome interaction map to determine the early molecular mechanisms of RPE apoptosis in AMD.

We have built a comprehensive interaction map by combining several independent sets of *in vivo* and *in vitro* data including immunoprecipitation, co-expression, protein domain, and published data from the literature. A large scale phosphorylation analysis demonstrated that multiple phosphorylation motifs are implicated in the mechanisms of AMD. A combination of phosphopeptide enrichment, high performance liquid chromatography, and electrospray tandem mass spectrometry, followed by database search, provides an integrated phosphoproteome showing the apoptotic pathway, energy metabolism, inflammation, cytoskeletal rearrangement, and mitochondrial network in AMD.

2 MATERIALS AND METHODS

2.1 Animals

We followed the NIH Guide and the Association for Research in Vision and Ophthalmology (ARVO) statement for *in vivo* experiments. The animal protocol was approved by the Institutional Animal Care and Use Committee.

Sprague-Dawley (SD) rats (male, 250-300 g) and mice (C57/BL6J genetic background) were purchased from Charles River Laboratories (Wilmington, MA). As a positive control for oxidative stress in the retina, diabetic condition was induced by intravenous injection of streptozotocin (65 mg/kg in 0.1M sodium citrate, pH 4.5, Sigma-Aldrich, St. Louis, MO). Negative control animals received injections of vehicle alone. Rats and mice (n=9, biological triplicate and technical triplicate) were considered to be diabetic at blood sugar levels >350 mg/dL. Animals were euthanized 2 or 4 weeks following onset of diabetes by an overdose of anesthetic. Comparative analysis was conducted with an identical animal strain (SD). Control SD rats and mice were sacrificed at 12 weeks of age and aged SD rats and mice were sacrificed at 52 and 54 weeks of age. Retinas from rats and mice were removed and frozen in liquid nitrogen. Retinas from different subgroups were collected and prepared for biochemical analysis. All experiments were repeated (n=3 biological samples) with technical triplicate (n=3). Stat View software was used for statistical analysis. Statistical significance was analyzed using unpaired Students' test or variance (ANOVA) when appropriate. The significance level $P < 0.05$ is considered as statistically significant.

2.2 Donor Eye Tissue and Phosphoprotein Enrichment

Human postmortem donor eye tissues were used following the tenets of the Declaration of Helsinki. Diabetic retinopathy (DR) human retinal tissues (n=9, biological triplicate x technical triplicate) were obtained from the Georgia Eye Bank (Atlanta, GA,). Human age-related macular degeneration (AMD) retina (8 mm macular and peripheral punches), RPE (8 mm central and peripheral punches), and age-matched control eyes (n=9, biological triplicate x technical triplicate) were provided by the Lions Eye Bank (Moran Eye Center, University of Utah). Phophoproteome of macular (I), peripheral retina (II), central RPE (III), and peripheral RPE (IV) were compared to age-matched control donor eyes to determine region-specific, senescence-associated molecular mechanisms during AMD progression. Phosphoproteins were enriched by charge-based spin column chromatography and resolved by 2D gel electrophoresis as previously reported [12]. In addition, trypsin digested phosphopeptides from whole lysates were enriched using Ga^{3+}/TiO_2 immobilized metal ion chromatography. Eluted phosphopeptides were analyzed using MALDI-TOF-TOF and ESI MS/MS. Serine, threonine, and tyrosine phosphorylations were confirmed by phospho-Western blotting analysis (data not shown).

2.3 ARPE-19 and HRP Cells

For *in vitro* experiments, retinal pigment epithelial cells (ARPE-19) were purchased from ATCC (Manassas, VA) and retinal progenitor cells (HRP) were kindly donated by Dr. Harold J. Sheeldo at the University of North Texas Health Science Center. ARPE-19 and HRP cells were cultured in a 5% CO_2 incubator at 37°C in 100 mm dishes (Nalge Nunc International, Naperville, IL) using Dulbecco's modified Eagle's medium (DMEM) with fetal bovine serum (10%) and penicillin/streptomycin (1%). Confluent cells were trypsinized (5-7 minutes at 37 °C) using a trypsin-EDTA buffer (0.1%, Sigma-Aldrich, St. Louis, MO), followed by centrifugation (300 x *g,* 7 min). Cells (eight to nine passages) were grown to confluence for 2–4 days and then were treated with H_2O_2 (200 µM), intense light (7,000-10,000 lux, 1-24 hrs) or constant light (700 lux, 48 hrs). HRP and ARPE-19 cells were rinsed (Modified Dulbecco's PBS) and lysed using IP lysis buffer containing Tris (25 mM), NaCl (150 mM), EDTA (1 mM), NP-40 (1%), glycerol (5%), and protease inhibitor cocktail at pH 7.4 by incubating

International Journal of Scientific & Engineering Research, Volume 8, Issue 2, February -2017
ISSN 2229-5518

on ice for 5 minutes with periodic sonication (3 × 5 min), followed by centrifugation (13,000 × *g,* 10 minutes). Proteins (1 mg/ml, 200-400 μL) were loaded for immunoprecipitation and nonspecific bindings were avoided using control agarose resin cross-linked by 4% bead agarose. Amino-linked protein-A beads were used to immobilize antiprohibitin antibody with a coupling buffer (1 mM sodium phosphate, 150 mM NaCl, pH 7.2), followed by incubation (room temperature, 2 hrs) with sodium cyanoborohydride (3 μL, 5 M). Columns were washed using a washing buffer (1 M NaCl), and protein lysate was incubated in the protein A-antibody column with gentle rocking overnight at 4 °C. The unbound proteins were spun down as flowthrough, and the columns were washed three times using washing buffer to remove nonspecific binding proteins. The interacting proteins were eluted by incubating with elution buffer for 5 minutes at RT. The eluted proteins were equilibrated with Laemmli sample buffer (5X, 5% β-mercaptoethanol). Eluted proteins were separated using SDS–PAGE and stained using Coomassie blue (Pierce, IL) or silver staining kit (Bio-Rad, Hercules, CA). Immunoprecipitated proteins were reported previously[13] and were used to establish interactome in the current study.

2.4 Two Dimensional SDS-PAGE

Protein samples were purified by ReadyPrep 2-D Cleanup Kit (Bio-Rad, CA) and quantified using BCA protein assay kit (Pierce, Rockford, IL). 150 μg of protein was incubated in 200 μl of rehydration buffer (8 M urea, 2 M thiourea, 2% CHAPS and 50 mM DTT) supplemented with 0.5% destreak IPG buffer, pH 3-10 (GE healthcare, PA). Isoelectric focusing was carried out using 11 cm immobiline dry strips (Bio-Rad, CA) with a linear pH 3-10 and 4-7 gradients. Strips were rehydrated for 12 hrs at 20 °C. Proteins were separated by the Ettan IPGphor-3 (GE healthcare) using programmed voltage gradients at 20 °C for a total of 12 kVh (1 h at 500 V, 1 h at 1000 V, 2 hrs at 6000 V and 40 min at 6000 V). The IPG strips were reduced in equilibration buffer I (0.375 M Tris-HCl, pH 8.8, 6 M urea, 20% glycerol, 2% SDS, and 50 mM DTT) for 20 min at 25 °C and alkylated for 20 min in equilibration buffer II containing 150 mM iodoacetamide. The equilibrated strips were placed on top of polyacrylamide gels (8-16%, Bio-Rad, CA) and sealed with 1% agarose buffer. Proteins were visualized by Coomassie staining using Imperial Protein Stain (Pierce, Rockford, IL) and Western blot.

2.5 Mass Spectrometry Analysis

Protein bands were excised (1×1×1 mm). The Coomassie-stained or silver-stained gel pieces were incubated using a Coomassie destaining buffer (200 μL of 50% MeCN in 25 mM NH_4HCO_3, pH 8.0, room temperature, 20 minutes) or silver destaining buffer (50% of 30 mM potassium ferricyanide, 50% of 100 mM sodium thiosulfate, 5-10 minutes). The gel pieces were dehydrated (200 μL, MeCN) and vacuum-dried (Speed Vac, Savant, Holbrook, NY). Disulfide bonds were reduced by DTT (10 mM) in the NH_4HCO_3 buffer (100 mM) for 30 minutes at 56 ºC, and then were alkylated by iodoacetamide (55 mM) in the NH_4HCO_3 buffer (100 mM) for 20 minutes at room temperature in the dark. Proteins were digested using trypsin (13 ng/μL sequencing-grade from Promega, 37 °C, overnight) in NH_4HCO_3 (10 mM) containing MeCN (10%). The peptides were enriched using a buffer (50 μL of 50% MeCN in NH_4HCO_3, 5% formic acid, 20 minutes, 37 °C). Dried peptides were dissolved in a mass spectrometry sample buffer (5–10 μL, 75% MeCN in NH_4HCO_3, 1% trifluoroacetic acid). Alpha-cyano-4-hydroxycinnamic acid (5 mg/mL, MW 189.04, Sigma-Aldrich, St. Louis, MO) was freshly dissolved in a matrix buffer (50% MeCN, 50% NH_4HCO_3, 1% triflouroacetic acid) and centrifuged (13,000 x *g*, 5 minutes). The peptide-matrix mixtures (0.5 μL) were spotted onto the MALDI Plate (Ground steel, Bruker Daltonics, Germany). Mass spectrometer and all spectra were calibrated using the known peptide, trypsin (842.5099 Da, 2211.105 Da). The mass spectrum was recorded in 800–3000 Da range using Flex MALDI-TOF mass spectrometer (Bruker Daltonics, Germany, 70–75% laser intensity, 100–300 shots). Mass spectrometry data were analyzed using Flex analysis software (Bruker Daltonics, Germany). Peptides were analyzed using the Mascot software (Matrix Science) and NCBI/SwissProt database (zero mismatch cleavage, carbamidomethyl cysteine, methionine oxidation, 50-300 ppm mass tolerance, S/T/Y phosphorylation = 79 m/z search). Peptide identification was evaluated based on Mascot MOWSE score, number of matched peptides, and protein sequence coverage. MOWSE score is expressed as -10logP as a probability value to compute the composite probability P. The experimental details for the ESI MS/MS experiments were reported previously [14–16].

2.6 Prohibitin Interactome Map and Lipid Analysis

AMD and oxidative biomarkers interactome were established using protein-protein interaction map software and databases, including STRING 10.0 (http://string-db.org/), MIPS (http://mips.helmholtz-muenchen.de/proj/ppi/) and iHOP (http://www.ihop-net.org/UniPub/iHOP/). Proteins found in AMD or oxidative stress conditions were added to establish the AMD interactome. Protein interactions were presented using eight categories, including neighborhood (green), gene fusion (red), co-occurrence (dark blue), co-expression (black), binding experiments (purple), databases (blue), text mining (lime), and homology (cyan). Protein interactions were determined and confirmed by genomic context, high-throughput experiments, co-expression, and previous publications in Pubmed. Protein database analysis showed the region-specific phosphorylation of specific proteins in AMD eyes. The interactome between AMD proteome was compared to the retina/RPE proteome under stress conditions.

International Journal of Scientific & Engineering Research, Volume 8, Issue 2, February -2017
ISSN 2229-5518

Lipids were extracted from ARPE-19 cells using cholorform-methanol (2:1, v/v) and organic solvent was evaporated under a gentle nitrogen stream and dissolved in chloroform for analysis by HPLC and mass spectrometry.

3 Result and Discussion

3.1 Phosphoproteome Changes in AMD

To determine whether early biomarkers in the phosphoproteome may play crucial roles in the progression of apoptotic signaling in AMD, we introduced a system-wide, unbiased, and high-throughput approach to examine the global phosphoproteome and the AMD interactome using a phosphoproteome enrichment method and protein interaction mapping.

The phosphoproteome of macula (I), peripheral retina (II), central RPE (III), and peripheral RPE (IV) in AMD donor eyes were compared to age-matched control donor eyes to determine region-specific, senescence-associated protein phosphorylation during AMD progression (Figure 1). Phosphoproteins from four different tissues were collected by using Ga^{3+}-based column chromatography and analyzed by two-dimensional gel electrophoresis. Phosphoproteins were identified by trypsin digestion, followed by MALDI-TOF-TOF mass spectrometry analysis. Altered phosphoproteins from peripheral regions of the neural retina (II) in AMD eyes were identified as follows; transferrin, pyruvate kinase, enolase, unnamed protein (α2 macroglobulin MG1 domain), PAK S/T kinase, protein phosphatase (PP2A), GFAP, tyrosine protein kinase FES/FPS, dynamin-like protein, creatine kinase, and vimentin (Figure 2A, Supplement Table 1). The presence of these phosphoproteins implies that iron homeostasis, energy regeneration, glycolytic flux, and cytoskeletal structure could be affected during AMD progression. In contrast, altered phosphoproteins from peripheral RPE (IV) were ubiquinon oxidoreductase, inositol 1,4,5 triphosphate receptor, calponin, ankyrin repeat domain 30B, guanylate cyclase, sorting nexin, and coiled-coil domain protein 73. The above phosphoproteins suggest potential alterations of fast energy transition, oxidative damage, blood flow, physiological hypoxia, cGMP, and apical polarity in AMD (Figure 2B, Supplement Table 1).

Phosphopeptides were obtained by trypsin digestion, followed by enrichment protocol by using Ga^{3+}-immobilized ion chromatography to confirm specific phosphoproteins. Eluted phosphopeptides were analyzed using MALDI-TOF-TOF and ESI MS/MS (Supplement Table 2). Phosphopeptides from transferrin (S678, S409), unnamed protein containing MG1 domain (S140), M2-type pyruvate kinase (S437), WD repeat-containing protein 59 isoform 3 (S375, Y437), ankyrin repeat domain 30B (S592), and coiled coil domain containing protein 73 (S770) were analyzed to show domain-specific phosphorylation sites, suggesting that protein phosphorylation could be influenced by surrounding amino acid sequences.

To establish the protein interactome map in the neuroretina and RPE, bioinformatics in AMD, bioinformatic STRING 10.0 software was used to integrate interaction data quantitatively from the STRING database from a large number of organisms and tissues. The STRING database currently covers 9,643,763 proteins from 2,031 organisms. AMD biomarker interactome was established using 94 proteins from the current phosphoproteome and published AMD proteome in the STRING query (Figure 3).

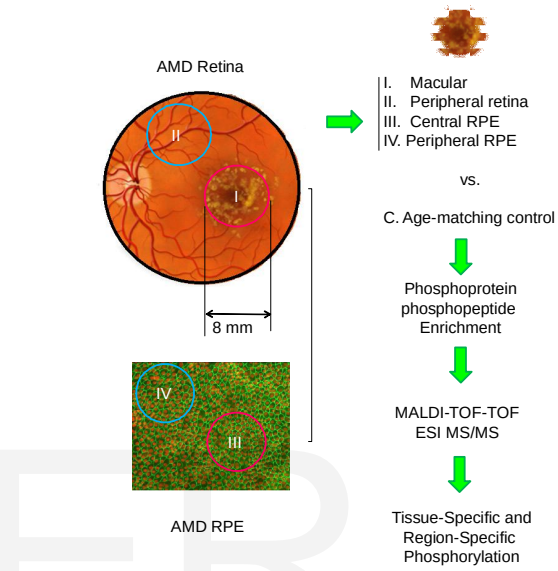

Fig. 1. The senescence-associated molecular events during AMD progression were identified by comparing the phosphoproteome of macular (I) and peripheral (II) neurosensory retina, central RPE (III) and peripheral RPE (IV) from AMD eyes and age-matching control eyes. Phosphoproteins were enriched by charge-based spin column chromatography and resolved by two-dimensional gel electrophoresis. Trypsin-digested phosphorylated peptides were enriched using Ga^{3+}/TiO_2 immobilized metal ion chromatography. Eluted phosphopeptides were analyzed by mass spectrometry. Statistical analysis and comparison show that altered phosphorylation signaling exists in AMD.

3.2 Oxidative Stress Mediated Protein Expression Profile in the RPE

Next, to determine phosphorylation signaling *in vitro*, ARPE19 cells were treated with 200µM H_2O_2 or intense or constant light. Proteins were extracted and separated by two-dimensional electrophoresis and visualized by Coomasie blue staining. Proteins from PBS-treated RPE cells or RPE cells grown in normal light conditions were separated in parallel to serve as a control. Gel image overlay revealed that 17 protein spots were up-regulated and 7 proteins spots were down-regulated as a result of the H_2O_2 treatment (Supplement Table 3, Supplement Table 5). Quantitative analysis of each spot under intense light (7,000-10,000 lux) or constant light (48 hours) based on normalized volume and intensity is listed in Supplement Table 3. Differentially expressed protein spots under various oxidative stress conditions were excised and digested by trypsin followed by protein identification using MALDI-

International Journal of Scientific & Engineering Research, Volume 8, Issue 2, February -2017
ISSN 2229-5518

TOF and MALDI-TOF-TOF mass spectrometry. Among these, retinoid metabolism related proteins, including RPE65, an all-trans-retinyl ester isomerohydrolase in the visual cycle, and retinol binding protein are of interest considering perturbed retinoid metabolism under oxidative stress in the RPE. Apoptotic (Annexin V) and redox reaction (GST) proteins were up-regulated and aging related (prohibitin) and respiratory (COX) proteins were down-regulated in RPE cells.

Potential biomarkers under oxidative stress were presented as an interaction network in Figure 4. Up- or down-regulated proteins under various stresses were added in STRING software query to establish a signaling network. The oxidative stress interactome showed potential connections between nuclear signaling (p53, BRCA1, ATM, SIRT1), oxygen-mediated apoptotic molecules (EPO, HIF, Bcl, BAD, TXN), and retrograde signaling (PHB, VDAC, EP300, RBP)-mediated reactions.

The analysis of AMD and oxidative stress interactomes revealed that 68-81% of protein signaling in AMD could be initiated from the oxidative stress biomarkers (Figure 3 and 4, Supplement Table 3). The protein interaction map-supported the idea that protein phosphorylation could be involved in apoptosisthe apoptotic or protective signaling in RPE cells. The AMD interactome (Figure 3) and oxidative stress biomarker interactome (Figure 4) suggest the following aspects of AMD: First, the AMD interactome indicated phosphocreatine shuttle atlterations, suggesting changes of ATP-requiring reactions in AMD, maintenance of high ATP/ADP ratio, and rhodopsin phosphorylation. Further, AMD may require increased Na^+/K^+ ATPase, phosphatidylinositol/inositol triphosphate signaling, and cGMP metabolism. Creatine kinase may induce pumping out Na^+ at night (dark) and blocking Na^+ during the day (light). Creatine kinase catalyzes the major energy demanding reaction, whereas pyruvate kinase may regulate the pigmentation and phagocytosis [17,18]. In addition, ATP synthase could be involved in mitochondrial dysfunction.

Second, GFAP is a retinal stress indicator, controlling blood-retina barrier breakdown and initial changes of Müller cells and the RPE. We observed chaperone changes, including crystalline, heat shock proteins, and albumin as well as changes in endogenous antioxidants such as peroxiredoxin and thioredoxin, suggesting increased oxidative stress, peroxiredoxin, and thioredoxin in AMD.

Third, changes in phosphorylation pattern of retinoid binding proteins such as CRABP, CRALBP, RDH, RGR, RPE65, and IRBP. Altered expressions of retinoid binding protein changes may lead to perturbation in circadian clock, which is also suggested by cytoskeletal remodeling through actin, vimentin, and tubulin phosphorylation [8,19,20]. Cytoskeletal modifications can also be associated with changes in extracellular matrix regulated by MMPs and angiogenic reactions mediated by VEGF and EPO. Fourth, AMD donor tissue exhibited apoptotic changes in peripheral RPE. In particular, peripheral mitochondria were disrupted by depleted prohibitin as a nuclear-mitochondrial shuttle in the RPE. Fifth, AMD interactome map suggests altered lipid metabolism that includes cardiolipin as a mitochondrial indicator of apoptosis and cholesterol as a protein aggregator. Sixth, complement activation by C3, C9, CFB, CFH, and CFI, is observed in AMD via vitronectin, clustrin, and plasminogen interaction.

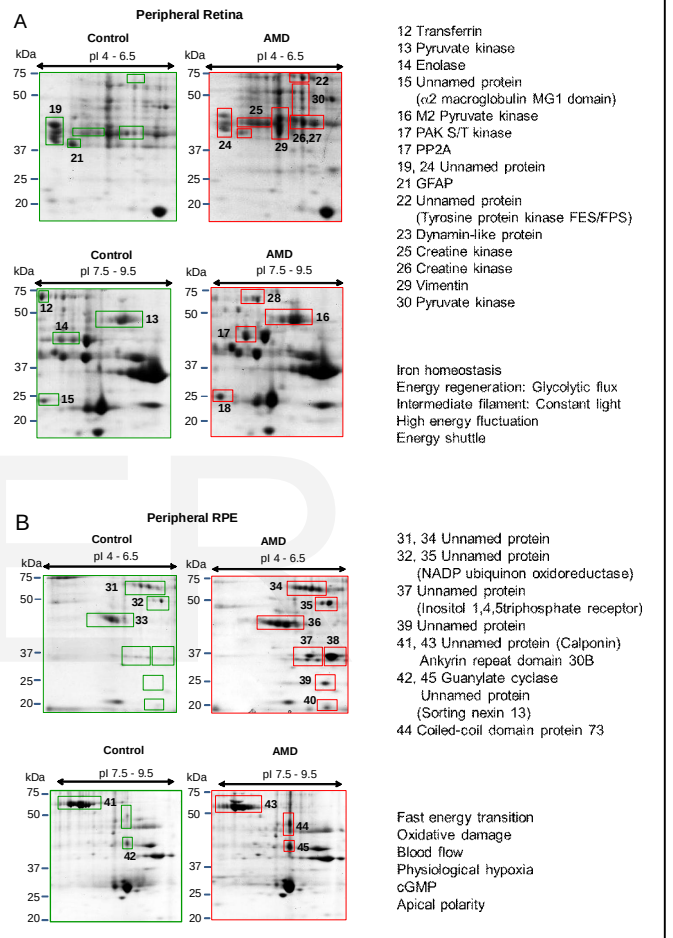

Fig. 2. **A.** Phosphoproteins from peripheral retina in AMD separated by 2D gel electrophoresis. Each spot represents Coomassie blue stained phosphoproteins (200 µg) from AMD eyes or age-matching control from the peripheral retinal region, which indicates the phosphorylation changes in AMD. Protein spots in the box represent identified proteins with altered phosphorylations. Y axis represents linear range of pI 4-6.5 and 7.5 to 9.5, and Y axis shows molecular weight (10-75 kDa). **B**. Phosphoproteins from retinal pigment epithelium (RPE) of AMD eyes separated by 2D gel electrophoresis. Each spot represents Coomassie blue stained phosphoproteins (200 µg) from the peripheral RPE region, which indicates the changes of phosphorylation signaling in AMD. Protein spots in the box represent identified protein by mass spectrometry analysis with altered phosphorylation. Y axis represents linear range of pI 4-6.5 and 7.5 to 9.5, and Y axis shows molecular weight (10-75 kDa).

3.3 Correlation between AMD Proteins and Oxidative

International Journal of Scientific & Engineering Research, Volume 8, Issue 2, February -2017
ISSN 2229-5518

Stress Biomarkers

We determined whether there was a positive correlation between early apoptotic biomarkers in RPE cells under oxidative stress and the phosphoproteome changes in AMD using our *in vitro* and *in vivo* data including ARPE19 cells, animal models, and human donor eyes from AMD patients (Supplement Table 3). In Figure 5, the AMD interactome and oxidative stress were connected together using STRING 10.0 software to analyze the molecular mechanisms involved in AMD progression in terms of oxidative stress, inflammation switch, energy metabolism, and transcriptional regulation. The new AMD interactome with oxidative biomarkers demonstrated that several earlier unrelated to AMD proteins, including ubiquitin, peroxiredoxin, MAP kinase, BUB 1/3, vimentin and crystalline are involved within the AMD progression, suggesting that cytoskeletal protein phosphorylation, crystalline aggregation, and mitochondrial signaling may contribute to RPE apoptosis. Then to confirm oxidative stress biomarkers, specific cytoskeletal protein changes were determined *in vivo* using animal model (C3H female mice, 7 weeks old). Neurofilament, vimentin, and β-tubulin were upregulated under 24 hours constant light compared to 12 hours dark/12 hours light condition (data now shown). To address the issue of lipid composition in RPE cells, we determined lipid changes under oxidative stress (Supplement Table 4, Supplement Table 5).

Our data demonstrated that longer chain fatty acid at sn-2 in phosphatidylcholine increased from 16 carbons to 24/26 carbons as well as cholesteryl esters under oxidative stress. The saturation of fatty acid in phosphatidylcholine also increased.

Based on our proteomics data that identified altered signaling of apoptosis in the retina and RPE, the pathological pathway determined by the AMD interactome could yield suitable targets for anti-apoptotic and anti-angiogenic therapy in Figure 6: (1) mitochondrial dysfunction in the peripheral RPE (prohibitin, ATP synthase); (2) oxidative stress including intense and constant light (peroxiredoxin, thioredoxin, glutathione S-transferase); (3) cytoskeletal remodeling by microtubule, actin filament, and intermediate filament (vimentin, actin, tubulin); (4) high concentration of nitric oxide (nitric oxide synthase);), (5) hypoxia (HIF1, erythropoietin, VEGF); (6) disrupted circadian clock (melatonin); (7) apoptotic downstream (pJAK2, pSTAT3, Bclxl, caspases); (8) altered lipid concentrations (cardiolipin, cholesterol); (9) altered visual cycle (CRABP, CRALBP, RPE65); (10) altered energy metabolism (S/T vs Y kinases, carnitine, pyruvate, ATP synthase); (11) aggregation of heat shock proteins and crystallins; and (12) inflammation (CFH, C3, collagen, vitronectin).

While the end point of apoptosis is well established, there is still a large gap between knowledge of early biochemical events and the end stage of AMD. Phosphoproteome changes under oxidative stress remain elusive in regard to the pathogenesis of AMD [21]. A detailed understanding of phosphorylation signaling in the RPE will answer how cytoskeletal reorganization and protein aggregation may control apoptosis and how we can intervene in the AMD apoptotic pathway.

Serial analysis of gene expression revealed 264 specific genes in rods, presenting a set of disease candidate genes and potential therapeutic targets. The set of rod-enriched genes suggested potential pathways in retinal biology, including electrophysiological responses of ion channels, phosphoinositide transfer, proteolysis, DNA damage repair, anti-oxidative enzymes, cytoskeletal components, and cadherins that bind nucleic acids [22]. Recently, cell-mediated immune response genes from RPE-choroid were identified in AMD [23,24]. Further, the top 20 genes as AMD biomarkers are predicted using a second donor cohort and a machine learning model. Transcriptome of human fetal RPE cells demonstrated that prolonged wound stimulus leads to passage-dependent altered expressions of the transcriptome, including TGF-β activators. Global expression profiling determined RPE specific genes, including the visual cycle proteins, transporters, epithelial channels, and cell adhesion molecules [25].

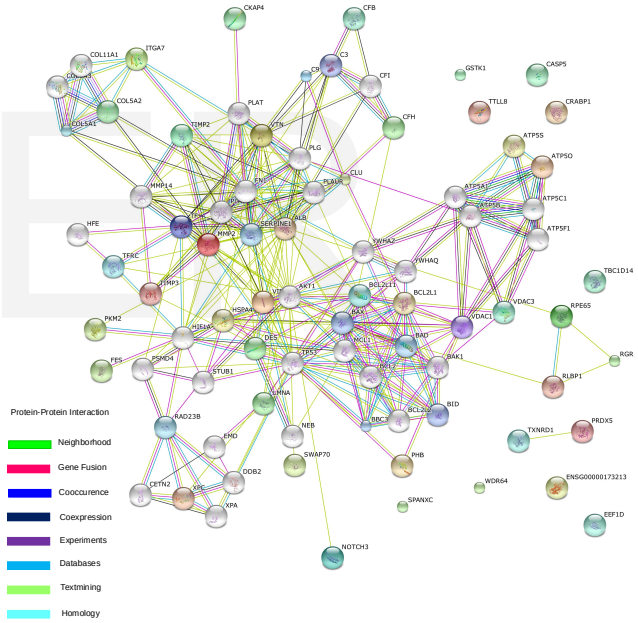

Fig. 3. AMD Biomarker Interactome. Potential AMD biomarkers are presented in the interaction map. Proteins found in AMD eyes were added in STRING software and determined protein interactions. Protein-protein interaction network was established by bioinformatic tools that include Osprey, VISANT, Navigator, STRING, iHOP, and Expasy protein databases. The interactome includes the direct (physical) and indirect (functional) protein associations. Interactions are derived from eight sources that include genomic context, high-throughput interaction experiments, conserved co-expression, and published knowledge in Pubmed and MiPS. The current interactome quantitatively integrates interaction data from the above sources for a large number of organisms, and transfers information between these organisms where applicable, from 9,643,763 proteins in 2,031 organisms. AMD biomarker interactome suggests that 68-81% of protein signaling in AMD could be initiated under oxidative stress. Interactions of complement factors (C3, C9, CFH, vitronectin), retinoid binding proteins (RPE65, RGR, RLBP), apoptotic molecules (Bcl2, BAD, BAX, BAK), energy metabolism related mitochondrial proteins (ATPase), transcription (p53), protease (MMP), cytoskeletal polymers (lamin, albumin), are noticed.

International Journal of Scientific & Engineering Research, Volume 8, Issue 2, February -2017
ISSN 2229-5518

Using reverse phase protein array, RPE exosomes showed signaling phosphoproteins under oxidative stress.[26] Stress-mediated exosome proteins are apoptosis and cell survival molecules, including Smac/Diablo, Akt, Src, ERK1/2, AMPK, and acetyl CoA carboxylate. The exosomes contain 38 phosphoproteins among 72 secreted proteins from RPE cells. This implies that the vesicle may have the potential to regulate signaling pathways in the retina and vitreous [26]. Mitochondrial complex I inhibition leads to increased autophagic markers and exocytotic activity, whereas decreased lysosomal activities in the RPE [27].

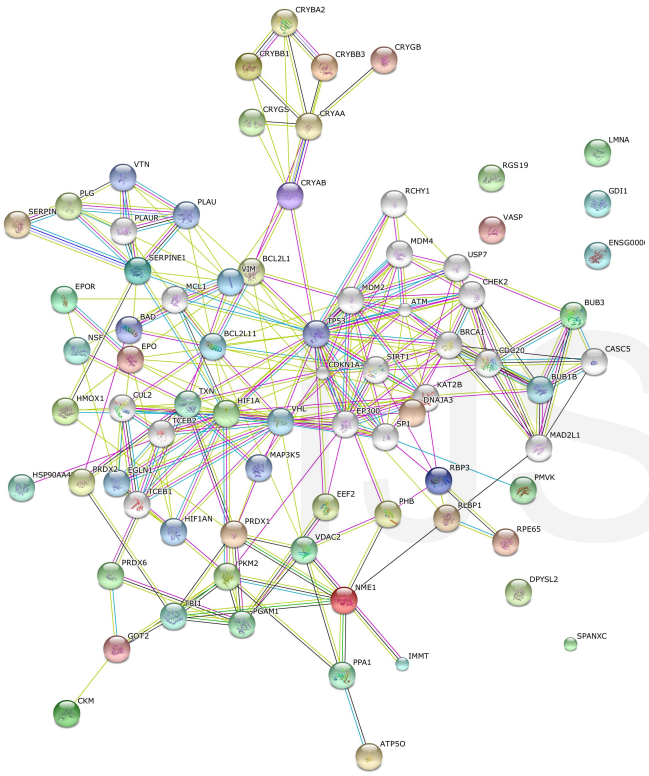

Fig. 4. Oxidative Stress Interactome. Potential biomarkers of oxidative stress in the retina and RPE were determined in the interaction map. Up- or down-regulated proteins under oxidative stress were added in STRING software and established protein interactions. Protein interactions between nuclear signaling (p53, BRCA1, ATM, SIRT1), oxygen-mediated apoptotic molecules (EPO, HIF, Bcl, BAD, TXN), and retrograde signaling (PHB, VDAC, EP300, RBP), were detected.

Our previous data suggested the potential cell death mechanisms in the retina and RPE under oxidative stress [8,9,12,13,16,28,29]. We demonstrated that oxidative stress may trigger induction of anti-apoptotic erythropoietin, JAK2, and BCL-xL, as well as pro-apoptotic caspases [19,28,30]. Oxidative stress also influenced mitochondrial-nuclear communication by shuttling mitochondrial prohibitin. In the current study, we observed that oxidative stress regulated phosphorylations of cytoskeletal and anti-apoptotic proteins, including vimentin and crystallin, may serve as the early protective mechanism. The cytoskeletal network formed by filamentous polymers, including vimentin, actin, and tubulin, determines how retinal and RPE cells respond to their extracellular environmental stimuli that include intense light (>7,000 lux) or constant light (>one week).

Further, our proteomic approach to understand RPE cell death under stress conditions demonstrated that: 1) crystallins are upregulated and hyperphosphorylated; 2) neuroprotective erythropoietin and subsequent JAK2 phosphorylations are tightly linked to a specific time after oxidative stress and in anticipation of daily light onset; 3) early signaling molecules, including mitochondrial prohibitin, changed their expression, subcellular localization, phosphorylation, and lipid interaction; 4) relative lipid compositions, including phosphatidylcholine and cholesterol, were altered under oxidative stress; and 5) oxidative stress leads to cytoskeletal reorganization through site-specific vimentin phosphorylations that regulate intermediate filaments, resulting in nonfilamentous particles [31]. Oxidative stress may influence the expression of genetic risk factors of AMD, including complement factor H (CFH). Although the potential importance of phosphorylation /dephosphorylation as a therapeutic target has been appreciated, no detailed approach to date has been made targeting biomarkers in phosphoproteome to treat ocular diseases [32,33]. For example, abnormalities in vimentin phosphorylation have been linked to neurodegenerative diseases, including AMD and Alzheimer's disease, but the vimentin phosphorylation network mechanism in RPE cells under oxidative stress remains largely unknown [18,34,35].

A general proteomic approach that includes protein identification by mass spectrometry has been used routinely for the last decade, however, RPE phosphoproteomics remains challenging due to the complexity, substoichiometry (not 100% phosphorylated), and kinetics (short vs. long time frame). Understanding phosphorylation reaction in AMD is not clear, because protein phosphorylation is a very dynamic process, while the aging process is slow.

Pioneering proteomic profiling studies revealed the human proteome, including drusen, lipofuscin [36–38], native differentiated/cultured dedifferentiated RPE proteome [39,40], AMD proteome [3,4,41], and diabetes [42]. Proteomic tools were used to study changes in the vitreous humor associated with diabetic retinopathy and retinal proteins in a glaucoma model [43]. Since oxidative stress is implicated in the etiology of several RPE diseases that include AMD, identification of molecular mediators and early signaling events under chronic stress is a crucial step for understanding cell death mechanism and retinal degeneration. However, limitations of proteomic approach, including minor proteins with low concentration, hydrophobic membrane proteins, reproducibility, and time

International Journal of Scientific & Engineering Research, Volume 8, Issue 2, February -2017
ISSN 2229-5518

and labor demanding processes, exist as hurdles to get comprehensive details on the molecular mechanism of AMD.

In Vitro vs. *In Vivo* Phosphorylation

Previous data demonstrated that Hsp70 (c-Jun N-terminal kinase), crystallins (Akt), and the increased expression of VDAC might be involved in AMD progression [3,18,44,45]. Altered phosphorylations of mitochondrial heat shock protein mtHsp70, αA/αB crystalline, vimentin, and ATP synthase were observed in RPE cell death under oxidative stress [16,46]. Retinoid binding proteins, including CRABP, RPE65, and RLBP1, could be involved in the advanced stages of AMD [10,47–50]. We observed altered lipid compositions that include increased carbon number of fatty acids, double bond saturation, higher cholesterol, and phosphatidylcholine, whereas cardiolipin levels decreased. Changes in lipid concentrations seem to diminish the membrane fluidity and accelerate protein aggregation [51–53].

In vivo data demonstrated that PP2A and vimentin are modulated by constant light and are key elements involved in cytoskeletal signaling in rd1 mutation model [8]. The expression levels of vimentin and PP2A are significantly increased when C3HeB/FeJ mice (rd1 allele; 12 weeks; photoreceptors degenerated) are exposed under continuous light for 7 days compared to a condition of 12h light/dark cycling exposure. When melatonin is administered to animals while they are exposed to continuous light, the increased levels of vimentin and PP2A return to a normal level. Further, vimentin has been shown to be a target of PP2A that directly binds vimentin and dephosphorylates it. Vimentin is present in all mesenchymal cells, and often used as a differentiation marker. Like other intermediate filaments, vimentin acts to maintain cellular integrity; however, vimentin may play a role in RPE survival by phosphorylation.

A positive correlation between the levels of PP2A and vimentin under light-induced stress suggests that cytoskeletal dynamics are regulated by vimentin phosphorylation. We postulate that light may induce post-translational modifications of vimentin and PP2Ac. We speculate that PP2Ac phosphorylation may control its subunit binding that determines its phosphatase activity and substrate specificity under stress conditions. Stabilized vimentin may act as an anti-apoptotic agent when cells are under stress.

The current interactome suggests that altered phosphoproteome interactions, including PP2A, pyruvate kinase, tyrosine kinase, and vimentin, exist in the retina and RPE in AMD. Phospho-Western blotting analysis revealed that phosphorylations of intermediate filament vimentin (Ser38, Ser55) and mitochondrial heat shock protein mt Hsp70 were modulated in the RPE *in vitro* [20]. Changes of vimentin phosphorylation are directed to reorganization of the intermediate filament network and altered function of RPE cells. The cytoskeletal network formed by filamentous proteins, including vimentin, determines how retinal and RPE cells respond to their extracellular environmental stimuli that include oxidative stress. Serine/threonine phosphatase PP2A-Cα/β (Tyr) and tubulin α1B/β2 were changed in the RPE, implying constant light-induced apoptosis signaling during AMD progression. Reducing the light-induced post-translational modification of vimentin and PP2A may assist to maintain the proper filament network in RPE cells.

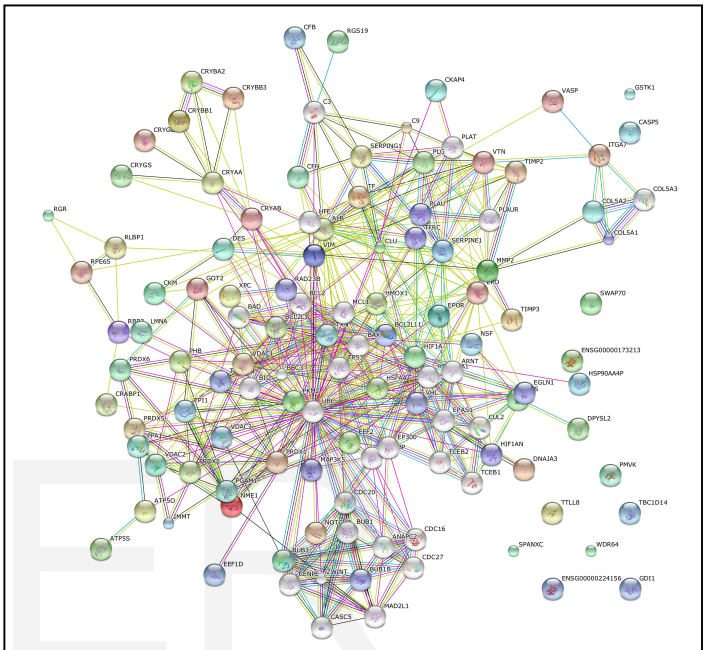

Fig. 5. The AMD interactome and oxidative stress biomarkers are presented in the integrated interaction map. AMD biomarkers and proteins under oxidative stress were submitted in STRING software query to establish comprehensive protein interactions in the retina and RPE to understand the early apoptotic reactions.

3.4 Mechanistic Dissection of AMD

Recently, the locations and functions of crystallins in the retina and RPE have been described [46,54–56]. αA- and αB-crystallin are located in the ganglion cell layer and photoreceptor layer, whereas β-crystallin is detected in all nuclear layers of the retina [57]. The functional roles of crystallins as chaperones, anti-apoptotic proteins, or signal transducers in the retina have also been described [54,57–59]. Phosphorylated αB-crystallin directly interacts with Bax and caspase-3 to suppress their pro-apoptotic action, and thus exerts a cytoprotective effect in the retina [59]. Light-induced up-regulation of αA-crystallin and increased phosphorylation of αA-crystallin in the aged retina have been reported. The specific function of each crystallin, particularly α/β-crystallin in the RPE, is still largely unknown, although levels of αB-crystallin are increased after heat shock and oxidative stress, and αB-crystallin immunoreactivity has been found in both rod outer segments

International Journal of Scientific & Engineering Research, Volume 8, Issue 2, February -2017
ISSN 2229-5518

and the RPE after light exposure [46,54,60].

Alterations in apoptosis and angiogenesis may lead to the pathological pathway which would be suited as targets for anti-apoptotic and anti-angiogenic therapy: (1) mitochondrial dysfunction in the peripheral RPE; (2) oxidative stress including intense and constant light; (3) cytoskeletal remodeling; (4) high concentration of nitric oxide; (5) hypoxia; (6) disrupted circadian clock; (7) pJAK2, pSTAT3, BclxL (8) altered lipid concentrations; (9) altered visual cycle; (10) altered energy metabolism (S/T vs Y kinases, carnitine, pyruvate); and (11) heat shock proteins, crystallins. Based on our proteomics data, we tested the following anti-apoptotic or anti-angiogenic molecules: (1) prohibitin (anti-apoptotic mitochondrial-nuclear shuttle), (2) erythropoietin (anti-apoptotic protein via JAK2/STAT3 pathway), (3) melatonin (anti-apoptotic and anti-angiogenic molecule protecting cytoskeletal reorganization through PP2A/vimentin pathway, (4) okadaic acid, arginine, and SNAP to control nitirc oxide concentration, (5) cardiolipin and cholesterol, (6) anthocyanin (anti-angiogenic via VEGFR2 pathway), (7) phospholipids, fatty acids, β-cyclodextrin to control lipids and cholesterol concentration [8,19].

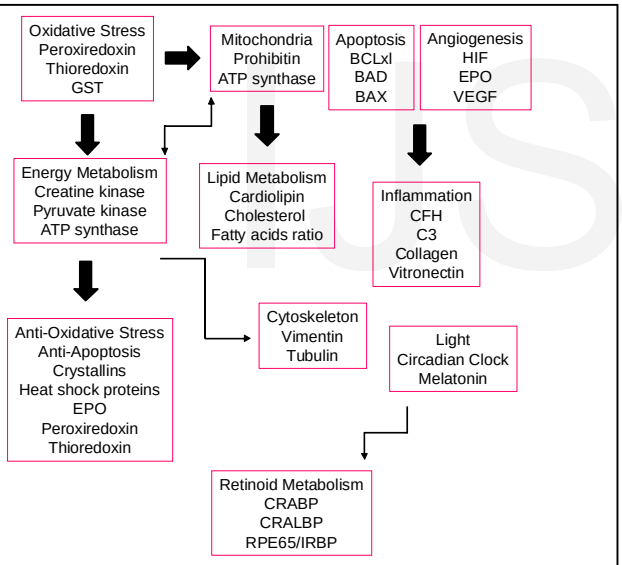

Fig. 6. Mechanistic dissection of AMD network. Based on our proteomics data, the potential AMD mechanism is proposed as follows: (1) mitochondrial dysfunction in the peripheral RPE (prohibitin, ATP synthase), (2) oxidative stress including intense and constant light (peroxiredoxin, thioredoxin, glutathione S-transferase), (3) cytoskeletal remodeling by microtubule, actin filament and intermediate filament (vimentin, actin, tubulin), (4) high concentration of nitric oxide (nitric oxide synthase, (5) hypoxia (HIF1, erythropoietin, VEGF), (6) disrupted circadian clock (melatonin), (7) apoptotic downstream (pJAK2, pSTAT3, Bclxl, caspases) (8) altered lipid concentrations (cardiolipin, cholesterol), (9) altered visual cycle (CRABP, CRALBP, RPE65), (10) altered energy metabolism (S/T vs Y kinases, carnitine, pyruvate, ATP synthase), (11) aggregation of heat shock proteins and crystallins, (12) inflammation (CFH, C3, collagen, vitronectin).

The current study determined the changes of phosphoproteome in peripheral retina and the RPE from AMD eyes *in vivo*. Our data suggests that changes in phosphoprotein levels in response to oxidative stress are mechanistically important. We propose that the AMD mechanism is induced by the changes of protein expressions and aggregations by membrane remodeling and lipid oxidation. Phosphoproteins in AMD *in vivo* were compared to oxidative stress biomarker in the retina/RPE *in vitro*. Previous observations of vimentin derived from human choroidal neovascular membranes in AMD, as well as in drusen and melanolipofuscin, support the positive correlation between biomarkers in RPE cells under stress and the AMD proteome [61,62].

Our phosphoproteomic interactome provides new insights regarding how phosphoproteome is related to cytoskeletal changes. In addition, the AMD interactome map elucidates the regulatory mechanism of apoptotic cell death governed by phosphorylation. These outcomes are expected to have an important positive impact because inhibition of target phosphorylation might be assigned as therapeutic intervention to serve the physiological role for the balanced phosphorylated cytoskeleton and chaperone in RPE cells.

Phosphorylation-dependent signaling could be different in various tissues, including the retina and the RPE, and may reflect the microenvironment diversity among ocular cells. Changes in the global phosphoproteome may be indicative of an early signaling event under oxidative stress conditions in the RPE. Increased longer chain fatty acids in phosphatidylcholine, cholesteryl esters, and phosphorylated crystalline could contribute to AMD progression, considering that drusen contain lipids and oxidized proteins such as crystallins. The aggregation mechanism by longer chain fatty acids and phosphorylated proteins may give insight into the molecular mechanism in AMD.

4 Conclusion

The current interactome map suggests that a positive correlation exists between early biomarkers of oxidative stress and phosphoproteins from AMD patients. The outcome of our work is the initial delineation of the underlying physiology of oxidative stress-mediated phosphorylation signaling in RPE apoptosis which can lead to AMD progression. In addition, the phosphoprotein interactome provides a stimulus for understanding oxidative stress-induced cytoskeletal changes and the mechanism of aggregate formation induced by protein phosphorylations. As a consequence, an effective therapeutic approach to treat AMD based on the modulation of phosphorylations are expected to result.

International Journal of Scientific & Engineering Research, Volume 8, Issue 2, February -2017
ISSN 2229-5518

Appendix 1. Supplement Table 1. AMD Proteome

Spot #	Protein identified	MOWSE score	% coverage	Mass	pI	Peptide #
12	transferrin	1.94e+12	28.7	76961	7.0	19
13	pyruvate kinase isozymes M1/M2 isoform e	195852	19.8	56274	8.7	8
14	2-phosphopyruvate-hydratase alpha-enolase	2.10e+10	28.6	47109	7.0	10
15	2-phosphopyruvate-hydratase alpha-enolase	7.22e+7	28.6	47109	7.0	10
16	M2-type pyruvate kinase	430810	15.8	57914	8.0	7
19	Unnamed (primary human renal epithelial cells)	1488	9.2	58545	8.7	4
21	Glial fibrillary acidic like protein	1.80e+10	38.8	47337	5.3	14
22	tyrosine-protein kinase Fes/Fps	448928	17.0	93779	6.3	11
22	receptor tyrosine kinase	412210	12.5	99657	6.9	7
23	Unnamed (Hsp70 protein)	219797	14.2	68116	5.3	7
23	dynamin-like protein Dymple isoform	5.08e+6	13.6	78062	6.3	7
25	creatine kinase, brain, isoform CRA_a	2.33e+6	27.3	42528	5.3	7
26	GAPIII (GTPase activating protein)	5.67e+6	12.0	96010	7.3	8
26	WD repeat-containing protein 59 isoform 3	2.38e+6	13.3	109801	8.0	7
27	Unnamed (intermediate filament head)	171525	18.0	47488	5.0	7
35	unnamed protein (NADH Ubiquinone oxidoreductase, 20 Kd subunit)	8961	34.5	22203	9.9	4
39	switch-associated protein 70	110691	8.0	68998	5.7	5
40	ankyrin repeat domain 30B	79.6	5.1	91935	5.9	5
43	Coiled coil domain containing protein 73	14699	12.8	92721	5.2	5
44	WD repeat-containing protein 64	92874	8.2	123627	6.7	5

Appendix 2. Supplement Table 2. Phosphorylated Peptides

Spot	Protein Identified	Potential modification	Peptide	Position
12	transferrin	Phosphorylation	CSTSSLLEACTFR	S678
			IMNGEADAMSLDGGFVYIAGK	S409
15	unnamed protein (MG1 domain)	Phosphorylation	IPITYNNGILFIHTDKPVYTPDQSVK	S140
16	M2-type pyruvate kinase	Phosphorylation	SAHQVAR	S437
26	WD repeat-containing protein 59	Phosphorylation	EDPPSSLLEEK	S375
			MLVTFPAQYPNNAAPSFQFINPTTITSAVK	Y437
43	ankyrin repeat domain 30B	Phosphorylation	LEESPVK	S592
44	coiled coil containing protein 73	Phosphorylation	AEPLISTVQQSHSQTVK	S770

Appendix 4. Supplement Table 4. Lipid Composition Changes in the RPE under Oxidative Stress

Control				Oxidative stress			
m/z	Rel. Int.	Lipid	Fatty acid	m/z	Rel.Int.	Lipid	Fatty acid
1543.8	22.09	phosphoethanolamine	18:1c9/20:1c11	637.3	33.74	phosphatidylglycerol	O-14:0/O-14:0
1465.9	18.2	glycerol, nonitol	32:08:00	734.6	30.29	phosphatidylcholine	12:0/20:0
1542.9	17.49	Phosphoethanolamine Salt	16:0/16:0	810.5	29.58	phosphatidylcholine	18:0/20:4c5,8,11,14
1549.9	14.87	phosphatidylcholine	18:0/18:1c9,12	1518.8	25.55	phosphatidylcholine	32:0/2-phy./2-phy.-Tet
298.8	14.37	sphingosine		808.6	25.31	phosphatidic acid	18:0/26:2y10,12
1508	14.16	phosphatidylcholine	14:0/20:4c5,8,11,14	762.7	21.25	phosphatidylcholine	10:0/24:0
734.6	13.74	phosphatidylcholine	12:0/20:0	902.6	20.71	phosphatidylcholine	18:0/26:0
808.6	13.54	phosphatidic acid	18:0/26:2y10,12	876.6	20.62	phosphatidylcholine	16:0/26:0
783.6	10.91	phosphatidylcholine	18:2c5,9/18:2c5,9	783.6	20.53	phosphatidylcholine	18:2c5,9/18:2c5,9
637.4	10.06	phosphatidylglycerol	O-14:0/O-14:0	836.6	19.2	phosphatidylethanolamine	22:6c4,7,10,13,16,19
639.6	1.7	cholesteryl ester	methyl palmitate	850.6	18.34	phosphatidylcholine	16:0/10:1pyr.10
651.5	1.55	cholesteryl ester	oleate	787.6	18.31	phosphatidylcholine	18:0/18:2c9,12
386.2	0.93	cholesterol		792.5	18.1	phosphatidylcholine	12:0/24:0
				651.6	5.02	cholesteryl ester	oleate
				639.5	3.93	cholesteryl ester	methyl palmitate
				386.1	1.83	cholesterol	

Appendix 3. Supplement Table 3. Comparison of AMD proteome and Oxidative Stress Biomarkers

AMD-related Proteome			Retina/RPE proteome under OS		
Protein	Model	Reference (category)	Protein	Model	Reference (category)
2-phosphopyruvate-hydratase alpha-enolase	AMD RPE	current study	Actin	RPE light	5(V)
2-phosphopyruvate-hydratase alpha-enolase	AMD RPE	current study	Actin	Retina proteome down melatonin	9(V)
Ankyrin repeat domain 30B	AMD RPE	current study	Alpha-crystallin A chain	Retina proteome down melatonin	9(III)
Annexin 5	AMD drusen	2(VI)	Alpha-crystallin A chain	Retina proteome down melatonin	9(III)
Annexin 5	RPE blebs	3(VI)	Alpha-crystallin A chain	Retina proteome down constant light	9(III)
Annexin 5	RPE secretome	6(VI)	Alpha-crystallin B chain	Retina proteome down melatonin	9(III)
Annexin 5	Melanolipofuscin	8(VI)	Alpha-crystallin B chain	Retina proteome down constant light	9(III)
ATP synthase	Melanolipofuscin	8(I)	Annexin 5	RPE proteome OS	4(VI)
ATP synthase b	AMD RPE	1(I)	Aspartate aminotransferase	Retina proteome down constant light	9(I)
Caspase 5	RPE secretome	7(VI)	ATP synthase	RPE light	5(I)
CHI	RPE secretome	7(VIII)	BCL-xl	Intense light	10(VI)
CHI	AMD secretome	7(VIII)	Beta-crystallin A1	Retina proteome down melatonin	9(III)
CHI	RPE secretome	7(VIII)	Beta-crystallin A1	Retina proteome down constant light	9(III)
CHI	AMD secretome	7(VIII)	Beta-crystallin A2	Retina proteome down melatonin	9(III)
Clusterin	AMD drusen	2(VI)	Beta-crystallin B1	Retina proteome down constant light	9(III)
Coiled coil domain containing protein 73	AMD RPE	current study	Beta-crystallin B3	Retina proteome down constant light	9(III)
Collagen a	AMD secretome	7(V)	Beta-crystallin S	Retina proteome down melatonin	9(III)
Complement C	RPE secretome	7(VIII)	Beta-soluble NSF attachment protein	Retina proteome down melatonin	9
Complement C	AMD secretome	7(VIII)	BUB3	RPE proteome OS	4
Complement component 9	AMD drusen	2(VIII)	Caspase 3	Intense light	10(VI)
CRABP	AMD retina	6(IV)	cFOS	Intense light	10
CRABP1	AMD RPE	1(IV)	CRALBP	RPE light	5
CRALBP	AMD RPE	1(IV)	Creatine kinase	RPE light	5(III)
creatine kinase, brain, isoform CRA_a	AMD RPE	current study	Crystallin aA	RPE light	5(III)
Crystallin aA	AMD RPE	1(III)	Crystallin aB	RPE light	5(III)
Crystallin aA	AMD retina	6(III)	Crystallin B1	RPE light	5(III)
Crystallin aB	AMD drusen	2(III)	Crystallin g	RPE light	5(III)
Crystallin aB	AMD retina	6(III)	Dihydropyrimidinase-related protein 2	Retina proteome up constant light	9
Crystallin aB	Melanolipofuscin	8(III)	Dihydropyrimidinase-related protein 2	Retina proteome down melatonin	9
Crystallin bA3	AMD drusen	2(III)	EF2	RPE proteome OS	4
Clusterin	AMD secretome	7(VI)	Erythropoietin	Circadian	10(V)
Cytoskeleton-associated protein 4	RPE blebs	3(V)	Erythropoietin receptor	Circadian	10(V)
Decorin	RPE blebs	3(V)	G binding protein b1	RPE light	5(I)
dynamin-like protein Dymple isoform	AMD RPE	current study	Gamma crystallin B	Retina proteome down constant light	9(III)
EF 1	RPE blebs	3	Gamma-crystallin F	Retina proteome down constant light	9(III)
EF4H	AMD RPE	1	GST-p	RPE proteome OS	4(I)
G binding protein	Melanolipofuscin	8(I)	Guanine binding protein	RPE proteome OS	4(I)
Galectin 3 BP	AMD secretome	7	Guanine nucleotide-binding protein G(I)/G(S)/G(T) subunit β-3	Retina proteome down melatonin	9(I)
GAPIII (GTPase activating protein)	AMD RPE	current study	Guanine nucleotide-binding protein G(o) subunit alpha	Retina proteome up constant light	9(I)
Glial fibrillary acidic like protein	AMD retina	current study	Guanine nucleotide-binding protein G(o) alpha	Retina proteome down melatonin	9(I)
GST	RPE blebs	3	HIF1A	Hypoxia retina/RPE	10
GSTp	AMD RPE	1	HO-1	Intense light RPE	10
GTPase Rab 14	RPE blebs	3(I)	HSP 70	RPE light	5(III)
Histone H2A2	AMD drusen	2	HSP 90	RPE light	5(III)
HSC 70	AMD RPE	1(III)	HSP 90 a	RPE proteome OS	4(III)
HSP 47	RPE secretome	7(III)	HSP b1	RPE proteome OS	4(III)
HSP 60	AMD RPE	1(III)	HSP b1	RPE light	5(III)
HSP 60	AMD retina	6(III)	Inorganic pyrophosphatase	Retina proteome down melatonin	9(I)
HSP 60	Melanolipofuscin	8(III)	IRBP	RPE light	5(IV)
HSP 70	AMD RPE	1(III)	Lamin A/C	RPE proteome OS	4(V)
HSP 70	Melanolipofuscin	8(III)	Mitochondrial inner membrane protein	Retina proteome down melatonin	9(VI)
HSP 70/88	RPE blebs	3(III)	Nucleoside diphosphate kinase A	Retina proteome up constant light	9(I)
HSP70	AMD retina	6(III)	Peroxiredoxin 1, 2	RPE proteome OS	4(III)
Keratin 7, 18	RPE blebs	3(V)	Peroxiredoxin-2	Retina proteome up constant light	9(III)
Lamin A/C	RPE blebs	3(V)	Peroxiredoxin-6	Retina proteome up constant light	9(III)
Laminin	RPE secretome	7(V)	Phosphoglycerate mutase 1	Retina proteome up constant light	9(I)
M2-type pyruvate kinase	AMD RPE	current study	Phosphomevalonate kinase	RPE proteome OS	4(I)
MMP-14	RPE blebs	3(V)	p38A2	Hypoxia	10(X)
MMP2	RPE secretome	7(V)	p38A2	Hyperoxia	10(X)
MMP2	AMD secretome	7(V)	p38A2	Intense light	10(X)
Mt HSP 75	AMD RPE	1(III)	Plasminogen	RPE light	5(X)
Peroxiredoxin 5	RPE blebs	3(III)	Plasminogen activator, inhibitor 1	RPE proteome OS	4(III)
Plasminogen activator inhibitor 1	RPE secretome	7	Prohibitin	RPE proteome OS	4(VI)
Prohibitin	Melanolipofuscin	8(VI)	Protein kinase 4	RPE light	5
Pyruvate kinase	AMD RPE	1(I)	Pyruvate kinase	RPE proteome OS	4(I)
pyruvate kinase isozymes M1/M2 isoform e	AMD retina	current study	Pyruvate kinase	RPE light	5(I)
RBP 3	Melanolipofuscin	8(IV)	Rab GDP dissociation inhibitor alpha	Retina proteome down constant light	9(I)
RDH 11	Melanolipofuscin	8(IV)	Rab GDP dissociation inhibitor alpha	Retina proteome down melatonin	9(I)
RDH 5	Melanolipofuscin	8(IV)	Retinaldehyde-binding protein 1	Retina proteome up constant light	9
RGR	Melanolipofuscin	8(IV)	Retinaldehyde-binding protein 1	Retina proteome down melatonin	9
RPE65	Melanolipofuscin	8(IV)	Retinol binding protein	RPE proteome OS	4
Serum albumin	AMD drusen	2(III)	RPE65	RPE proteome OS	4(IV)
switch-associated protein 70	AMD RPE	current study	RPE65	RPE light	5(IV)
Thioredoxin reductase 1	RPE blebs	3(III)	Ser/Thr-protein phosphatase 2A 65 kDa regulatory subunit A α	Retina proteome down constant light	9(I)
TIMP3	AMD drusen	2(X)	Ser/Thr-protein phosphatase 2A 65 kDa regulatory subunit A α	Retina proteome down melatonin	9(I)
transferrin	AMD retina	current study	Serum albumin precursor	Retina proteome down melatonin	9(III)
Tubulin	RPE blebs	3(V)	Thioredoxin	Intense light RPE	10(III)
Tubulin a	AMD retina	6(V)	Thioredoxin-dependent peroxide reductase 3	RPE proteome OS	4(III)
Tubulin a	Melanolipofuscin	8(V)	Triosephosphate isomerase	Retina proteome down constant light	9
Tubulin b	Melanolipofuscin	8(V)	Tubulin a1B	RPE light	5(V)
Tyrosine-protein kinase Fes/Fps	AMD retina	current study	Tubulin b2	RPE light	5(V)
Ubiquinone oxidoreductase, 20 Kd subunit	AMD RPE	current study	Tubulin beta-5 chain	Retina proteome up constant light	9(V)
Unnamed (Hsp70 protein)	AMD RPE	current study	VDAC2	RPE proteome OS	4(VI)
Unnamed (intermediate filament head)	AMD RPE	current study	Vesicle-fusing ATPase	Retina proteome up constant light	9(I)
Unnamed (primary human renal epithelial cells)	AMD RPE	current study	vimentin	Retina proteome up constant light	9(V)
Unnamed protein (NADH Ubiquinone oxidoreductase)	AMD RPE	current study	vimentin	Retina proteome down melatonin	9(V)
VDAC 1	AMD RPE	1(VI)			
VDAC 1, 2, 3	Melanolipofuscin	8(VI)			
VDAC1	AMD retina	6(VI)			
VDAC3	RPE blebs	3(VI)			
Vimentin	Melanolipofuscin	8(V)			
Vimentin	AMD drusen	2(V)			
Vitronectin	AMD drusen	2(X)			
WD repeat-containing protein 59 isoform 3	AMD retina	current study			
WD repeat-containing protein 64	AMD retina	current study			

References

1.[1]Nordmark et al., IOVS. 2006, 47, 815 [2]Crabb et al., PNAS. 2002, 12, 14682 [3] Alcazar et al., MCP. 2009, 8, 2201 [4] Arnouk et al., IOP. 2011, 74, 254 [5] Lee et al., IJBM. 2011, 48, 194
16.[1]Ebert et al., IOVS. 2006, 47, 2280 [7] An et al., JPR. 2006, 5, 2599 [8]Warburton et al., MV. 2007, 13, 318 [9] Chung et al., JNR. 2009, 87, 2365 [10] Zhang et al., IJBM. 2010, 47, 255

Category

I. Phosphocreatine Shuttle Changes in AMD
1. Changes of ATP-requiring reactions in AMD
2. Maintenance of high ATP/ADP ratio
3. Rhodopsin phosphorylation
4. Na^+/K^+ ATPase
5. Phosphatidylinositol/inositol triphosphate signaling
6. cGMP metabolism
7. Pumping out Na^+ (night), blocking Na^+ (day)
8. Creatine kinase (major energy source)vs. pyruvate kinase (pigmentation, phagocytosis) vs. ATP synthase (mitochondrial dysfunction)

II. GFAP as a Retinal Stress Indicator
1. Blood-retinal barrier breakdown
2. Initial changes of Müller cell and RPE

III. Chaperone Changes
1. Crystalline, heat shock proteins
2. Albumin
3. Oxidative stress, peroxiredoxin, thioredoxin

IV. Altered Retinoid Metabolism
1. CRABP, CRALBP
2. RDH, IGR, RPE65, IRBP

V. Circadian Clock
1. Vimentin, PP2A
2. Cytoskeletal remodeling, tubulin, phosphorylation changes
3. Extracellular matrix, MMP, angiogenesis, EPO

VI. Apoptotic Peripheral RPE
1. Prohibitin as a nuclear/mitochondrial shuttle in the retina/RPE
2. Lipid binding/switch
2. Mitochondrial dysfunction

VII. Lipid Metabolism
1. Cardiolipin as a mitochondrial indicator of apoptosis
2. Cholesterol as an aggregator
3. Fatty acids balance

VIII. Complement Activation

IX. Unknown Proteins
1. Unnamed proteins
2. Homologous proteins

X. RPE Aging
1. Protein fragmentation, aggregation
2. Retina overproliferation vs. RPE apoptosis

International Journal of Scientific & Engineering Research, Volume 8, Issue 2, February -2017
ISSN 2229-5518

Appendix 5. Supplement Table 5. AMD Interactome vs. Oxidative Stress Biomarkers

AMD Interactome in Figure 3

1. MMP2 matrix metallopeptidase 2 (gelatinase A, 72kDa gelatinase, 72kDa type IV collagenase); In addition to gelatin and collagens, it cleaves KiSS1 at a Gly- | - Leu bond (660 aa)
2. VIM vimentin; Vimentins are class - III intermediate filaments found in various non - epithelial cells, especially mesenchymal cells (466 aa)
3. VTN vitronectin; Vitronectin is a cell adhesion and spreading factor found in serum and tissues. Vitronectin interact with glycosaminoglycans and proteoglycans. Is recognized by certain members of the integrin family and serves as a cell - to - substrate adhesion molecule. Inhibitor of the membrane - damaging effect of the terminal cytolytic complement pathway (478 aa)
4. ITGA7 integrin, alpha 7; Integrin alpha - 7/beta - 1 is the primary laminin receptor on skeletal myoblasts and adult myofibers. During myogenic differentiation, it may induce changes in the shape and mobility of myoblasts, and facilitate their localization at laminin - rich sites of secondary fiber formation. It is involved in the maintenance of the myofibers cytoarchitecture as well as for their anchorage, viability and functional integrity. Isoform Alpha - 7X2B and isoform Alpha - 7X1B promote myoblast migration on laminin 1 and laminin 2/4, but isoform Alpha - 7X1B is less active on laminin 1 (In vitro) (1137 aa)
5. RPE65 retinal pigment epithelium - specific protein 65kDa; Plays important roles in the production of 11 - cis retinal and in visual pigment regeneration. The soluble form binds vitamin A (all - trans - retinol), making it available for LRAT processing to all - trans - retinyl ester. The membrane form, palmitoylated by LRAT, binds all - trans retinyl esters, making them available for IMH (isomerohydrolase) processing to all - cis - retinol. The soluble form is regenerated by transferring its palmitoyl groups onto 11 - cis - retinol, a reaction catalyzed by LRAT. (533 aa)
6. TIMP2 TIMP metallopeptidase inhibitor 2; Complexes with metalloproteinases (such as collagenases) and irreversibly inactivates them. Known to act on MMP - 1, MMP - 2, MMP - 3, MMP - 7, MMP - 8, MMP - 9, MMP - 10, MMP - 13, MMP - 14, MMP - 15, MMP - 16 and MMP - 19 (220 aa) NOTCH3 Notch homolog 3 (Drosophila); Functions as a receptor for membrane - bound ligands Jagged1, Jagged2 and Delta1 to regulate cell - fate determination. Upon ligand activation through the released notch intracellular domain (NICD) it forms a transcriptional activator complex with RBP- J kappa and activates genes of the enhancer of split locus. Affects the implementation of differentiation, proliferation and apoptotic programs (By similarity) (2321 aa)
7. C9 complement component 9; Constituent of the membrane attack complex (MAC) that plays a key role in the innate and adaptive immune response by forming pores in the plasma membrane of target cells. C9 is the pore - forming subunit of the MAC (559 aa)
8. TF transferrin; Transferrins are iron binding transport proteins which can bind two Fe(3+) ions in association with the binding of an anion, usually bicarbonate. It is responsible for the transport of iron from sites of absorption and heme degradation to those of storage and utilization. Serum transferrin may also have a further role in stimulating cell proliferation (698 aa)
9. VDAC1 voltage - dependent anion channel 1 pseudogene 1; Forms a channel through the mitochondrial outer membrane and also the plasma membrane. The channel at the outer mitochondrial membrane allows diffusion of small hydrophilic molecules; in the plasma membrane it is involved in cell volume regulation and apoptosis. It adopts an open conformation at low or zero membrane potential and a closed conformation at potentials above 30 - 40 mV. The open state has a weak anion selectivity whereas the closed state is cation selective. May participate in the formation of the permeability transition pore. (283 aa)
10. PRDX5 peroxiredoxin 5; Reduces hydrogen peroxide and alkyl hydroperoxides with reducing equivalents provided through the thioredoxin system. Involved in intracellular redox signaling (214 aa) TIMP3 TIMP metallopeptidase inhibitor 3; Complexes with metalloproteinases (such as collagenases) and irreversibly inactivates them. May form part of a tissue - specific acute response to remodeling stimuli. Known to act on MMP - 1, MMP - 2, MMP - 3, MMP - 7, MMP - 9, MMP - 13, MMP - 14 and MMP - 15 (211 aa)
11. TTLL8 tubulin tyrosine ligase - like family, member 8; Monoglycylase which modifies both tubulin and non - tubulin proteins, generating side chains of glycine on the gamma - carboxyl groups of specific glutamate residues of target proteins. Monoglycylates tubulin, with a preference for alpha - tubulin toward beta - tubulin. Has the ability to modify non -tubulin proteins such as ANP32A, ANP32B, SET and NCL. Involved in the side - chain initiation step of the glycylation reaction by adding a single glycine chain to generate monoglycine side chains. Not involved in elongation step of the polyglycylation (834 aa)
12. RLBP1 retinaldehyde binding protein 1; Carries 11 - cis - retinol and 11 - cis - retinaldehyde as endogenous ligands and may be a functional component of the visual cycle (317 aa)
13. XPC xeroderma pigmentosum, complementation group C; Involved in DNA excision repair. May play a part in DNA damage recognition and/or in altering chromatin structure to allow access by damage - processing enzymes (940 aa)
14. ATP5O ATP synthase, H+ transporting, mitochondrial F1 complex, O subunit; Mitochondrial membrane ATP synthase (F(1)F(0) ATP synthase or Complex V) produces ATP from ADP in the presence of a proton gradient across the membrane which is generated by electron transport complexes of the respiratory chain. F -type ATPases consist of two structural domains, F(1) - containing the extramembraneous catalytic core and F(0) - containing the membrane proton channel, linked together by a central stalk and a peripheral stalk. During catalysis, ATP synthesis in the catalytic domain of F(1) is coupled (213 aa)
15. ALB albumin; Serum albumin, the main protein of plasma, has a good binding capacity for water, Ca(2+), Na (+), K(+), fatty acids, hormones, bilirubin and drugs. Its main function is the regulation of the colloidal osmotic pressure of blood (609 aa)
16. CRABP1 cellular retinoic acid binding protein 1; Cytosolic CRABPs may regulate the access of retinoic acid to the nuclear retinoic acid receptors (137 aa)
17. PHB prohibitin; Prohibitin inhibits DNA synthesis. It has a role in regulating proliferation. As yet it is unclear if the protein or the mRNA exhibits this effect. May play a role in regulating mitochondrial respiration activity and in aging (272 aa)
18. BCL2L1 BCL2 - like 1; Potent inhibitor of cell death. Isoform Bcl - X(L) anti - apoptotic activity is inhibited by association with SIVA isoform 1. Inhibits activation of caspases (By similarity). Appears to regulate cell death by blocking the voltage - dependent anion channnel (VDAC) by binding to it and preventing the release of the caspase activator, cytochrome c, from the mitochondrial membrane. The Bcl - X(S) isoform promotes apoptosis (233 aa) HSPA4 heat shock 70kDa protein 4 (840 aa)

International Journal of Scientific & Engineering Research, Volume 8, Issue 2, February -2017
ISSN 2229-5518

19. ATP5S ATP synthase, H+ transporting, mitochondrial F0 complex, subunit s (factor B); Involved in regulation of mitochondrial membrane ATP synthase. Necessary for H(+) conduction of ATP synthase (215 aa)
20. ENSG00000173213 Tubulin beta - 8 chain B ; Tubulin is the major constituent of microtubules. It binds two moles of GTP, one at an exchangeable site on the beta chain and one at a non - exchangeable site on the alpha - chain (By similarity) (444 aa)
21. CLU clusterin; It is known to be expressed in a variety of tissues and it seems to be able to bind to cells, membranes and hydrophobic proteins. It has been associated with programmed cell death (apoptosis) (501 aa)
22. SWAP70 SWAP switching B - cell complex 70kDa subunit; Phosphatidylinositol 3,4,5 -trisphosphate - dependent guanine nucleotide exchange factor (GEF) which, independently of RAS, transduces signals from tyrosine kinase receptors to RAC. It also mediates signaling of membrane ruffling. Regulates the actin cytoskeleton as an effector or adapter protein in response to agonist stimulated phosphatidylinositol (3,4) - bisphosphate production and cell protrusion (By similarity) (585 aa)
23. PKM2 pyruvate kinase, muscle; Glycolytic enzyme that catalyzes the transfer of a phosphoryl group from phosphoenolpyruvate (PEP) to ADP, generating ATP. Stimulates POU5F1 - mediated transcriptional activation. Plays a general role in caspase independent cell death of tumor cells. The ratio betwween the highly active tetrameric form and nearly inactive dimeric form determines whether glucose carbons are channeled to biosynthetic processes or used for glycolytic ATP production. The transition between the 2 forms contributes to the control of glycolysis and is important for tumor cell proliferation (531 aa)
24. FES feline sarcoma oncogene (822 aa)
25. WDR64 WD repeat domain 64 (634 aa)
26. SPANXC SPANX family, member C (97 aa)
27. RGR retinal G protein coupled receptor; Receptor for all - trans - and 11 - cis - retinal. Binds preferentially to the former and may catalyze the isomerization of the chromophore by a retinochrome - like mechanism (295 aa)
28. CFH complement factor H; Factor H functions as a cofactor in the inactivation of C3b by factor I and also increases the rate of dissociation of the C3bBb complex (C3 convertase) and the (C3b)NBB complex (C5 convertase) in the alternative complement pathway (1231 aa)
29. LMNA lamin A/C; Lamins are components of the nuclear lamina, a fibrous layer on the nucleoplasmic side of the inner nuclear membrane, which is thought to provide a framework for the nuclear envelope and may also interact with chromatin. Lamin A and C are present in equal amounts in the lamina of mammals (664 aa)
30. DES desmin; Desmin are class - III intermediate filaments found in muscle cells. In adult striated muscle they form a fibrous network connecting myofibrils to each other and to the plasma membrane from the periphery of the Z - line structures (470 aa)
31. COL5A2 collagen, type V, alpha 2; Type V collagen is a member of group I collagen (fibrillar forming collagen). It is a minor connective tissue component of nearly ubiquitous distribution. Type V collagen binds to DNA, heparan sulfate, thrombospondin, heparin, and insulin. Type V collagen is a key determinant in the assembly of tissue - specific matrices (By similarity) (1499 aa)
32. CKAP4 cytoskeleton - associated protein 4 (602 aa)
33. GSTK1 glutathione S -transferase kappa 1; Significant glutathione conjugating activity is found only with the model substrate, 1 - chloro - 2,4 - dinitrobenzene (CDNB) (282 aa)
34. CASP5 caspase 5, apoptosis - related cysteine peptidase; Mediator of programmed cell death (apoptosis) (447 aa)
35. TBC1D14 TBC1 domain family, member 14; May act as a GTPase - activating protein for Rab family protein(s) (By similarity) (693 aa)
36. CFB complement factor B (621 aa) VDAC3 voltage - dependent anion channel 3; Forms a channel through the mitochondrial outer membrane that allows diffusion of small hydrophilic molecules (By similarity) (284 aa)
37. EEF1D eukaryotic translation elongation factor 1 delta (guanine nucleotide exchange protein); EF- 1 - beta and EF - 1 delta stimulate the exchange of GDP bound to EF - 1 - alpha to GTP (647 aa)
38. TXNRD1 thioredoxin reductase 1; Isoform 1 may possess glutaredoxin activity as well as thioredoxin reductase activity and induces actin and tubulin polymerization, leading to formation of cell membrane protrusions. Isoform 4 enhances the transcriptional activity of estrogen receptors alpha and beta while isoform 5 enhances the transcriptional activity of the beta receptor only. Isoform 5 also mediates cell death induced by a combination of interferon - beta and retinoic acid (651 aa)

AMD Interactome and OS Biomarkers in Figure 4, Figure 5

1. NME1 non - metastatic cells 1, protein (NM23A) expressed in; Major role in the synthesis of nucleoside triphosphates other than ATP. Possesses nucleoside - diphosphate kinase, serine/threonine - specific protein kinase, geranyl and farnesyl pyrophosphate kinase, histidine protein kinase and 3' - 5' exonuclease activities. Involved in cell proliferation, differentiation and development, signal transduction, G protein - coupled receptor endocytosis, and gene expression. Required for neural development including neural patterning and cell fate determination. Has tumor metastasis - suppressive capacity (177 aa)
2. CRYBB3 crystallin, beta B3; Crystallins are the dominant structural components of the vertebrate eye lens (211 aa)
3. CRYBB1 crystallin, beta B1; Crystallins are the dominant structural components of the vertebrate eye lens (252 aa)
4. HMOX1 heme oxygenase (decycling) 1; Heme oxygenase cleaves the heme ring at the alpha methene bridge to form biliverdin. Biliverdin is subsequently converted to bilirubin by biliverdin reductase. Under physiological conditions, the activity of heme oxygenase is highest in the spleen, where senescent erythrocytes are sequestrated and destroyed (288 aa)
5. MMP2 matrix metallopeptidase 2 (gelatinase A, 72kDa gelatinase, 72kDa type IV collagenase); In addition to gelatin and collagens, it cleaves KiSS1 at a Gly- | - Leu bond (660 aa)
6. CKM creatine kinase, muscle; Reversibly catalyzes the transfer of phosphate between ATP and various phosphogens (e.g. creatine phosphate). Creatine kinase isoenzymes play a central role in energy transduction in tissues with large, fluctuating energy demands, such as skeletal muscle, heart, brain and spermatozoa (381 aa)
7. EPOR erythropoietin receptor; Receptor for erythropoietin. Mediates erythropoietin - induced erythroblast proliferation and differentiation. Upon EPO stimulation, EPOR dimerizes triggering the JAK2/STAT5 signaling cascade. In some cell types, can also activate STAT1 and STAT3. May also activate the LYN tyrosine kinase (508 aa)

International Journal of Scientific & Engineering Research, Volume 8, Issue 2, February -2017
ISSN 2229-5518

8. SERPINE1 serpin peptidase inhibitor, clade E (nexin, plasminogen activator inhibitor type 1), member 1; This inhibitor acts as 'bait' for tissue plasminogen activator, urokinase, and protein C. Its rapid interaction with TPA may function as a major control point in the regulation of fibrinolysis (402 aa)
9. VIM vimentin; Vimentins are class - III intermediate filaments found in various non - epithelial cells, especially mesenchymal cells (466 aa)
10. RBP3 retinol binding protein 3, interstitial; IRBP shuttles 11 - cis and all trans retinoids between the retinol isomerase in the pigment epithelium and the visual pigments in the photoreceptor cells of the retina (1247 aa)
11. VTN vitronectin; Vitronectin is a cell adhesion and spreading factor found in serum and tissues. Vitronectin interact with glycosaminoglycans and proteoglycans. Is recognized by certain members of the integrin family and serves as a cell - to - substrate adhesion molecule. Inhibitor of the membrane - damaging effect of the terminal cytolytic complement pathway (478 aa)
12. CRYAB crystallin, alpha B; May contribute to the transparency and refractive index of the lens (175 aa)
13. GOT2 glutamic- oxaloacetic transaminase 2, mitochondrial (aspartate aminotransferase 2); Facilitates cellular uptake of long - chain free fatty acids (430 aa)
14. VASP vasodilator- stimulated phosphoprotein; Ena/VASP proteins are actin - associated proteins involved in a range of processes dependent on cytoskeleton remodeling and cell polarity such as axon guidance, lamellipodial and filopodial dynamics, platelet activation and cell migration. VASP promotes actin filament elongation. It protects the barbed end of growing actin filaments against capping and increases the rate of actin polymerization in the presence of capping protein. VASP stimulates actin filament elongation by promoting the transfer of profilin - bound actin monomers onto the barbed end [...] (380 aa)
15. EPO erythropoietin; Erythropoietin is the principal hormone involved in the regulation of erythrocyte differentiation and the maintenance of a physiological level of circulating erythrocyte mass (193 aa)
16. ITGA7 integrin, alpha 7; Integrin alpha - 7/beta - 1 is the primary laminin receptor on skeletal myoblasts and adult myofibers. During myogenic differentiation, it may induce changes in the shape and mobility of myoblasts, and facilitate their localization at laminin - rich sites of secondary fiber formation. It is involved in the maintenance of the myofibers cytoarchitecture as well as for their anchorage, viability and functional integrity. Isoform Alpha - 7X2B and isoform Alpha - 7X1B promote myoblast migration on laminin 1 and laminin 2/4, but isoform Alpha - 7X1B is less active on laminin 1 (In vitro) (1137 aa)
17. CRYGB crystallin, gamma B; Crystallins are the dominant structural components of the vertebrate eye lens (175 aa)
18. RPE65 retinal pigment epithelium - specific protein 65kDa; Plays important roles in the production of 11 - cis retinal and in visual pigment regeneration. The soluble form binds vitamin A (all - trans - retinol), making it available for LRAT processing to all - trans - retinyl ester. The membrane form, palmitoylated by LRAT, binds all - trans retinyl esters, making them available for IMH (isomerohydrolase) processing to all - cis - retinol. The soluble form is regenerated by transferring its palmitoyl groups onto 11 - cis - retinol, a reaction catalyzed by LRAT. The enzymatic activity is linearly dependent of th [...] (533 aa)
19. DNAJA3 DnaJ (Hsp40) homolog, subfamily A, member 3; Modulates apoptotic signal transduction or effector structures within the mitochondrial matrix. Affect cytochrome C release from the mitochondria and caspase 3 activation, but not caspase 8 activation. Isoform 1 increases apoptosis triggered by both TNF and the DNA - damaging agent mytomycin C; in sharp contrast, isoform 2 suppresses apoptosis. Can modulate IFN gamma - mediated transcriptional activity (480 aa)
20. PRDX1 peroxiredoxin 1; Involved in redox regulation of the cell. Reduces peroxides with reducing equivalents provided through the thioredoxin system but not from glutaredoxin. May play an important role in eliminating peroxides generated during metabolism. Might participate in the signaling cascades of growth factors and tumor necrosis factor- alpha by regulating the intracellular concentrations of H(2)O(2). Reduces an intramolecular disulfide bond in GDPD5 that gates the ability to GDPD5 to drive postmitotic motor neuron differentiation (199 aa)
21. TIMP2 TIMP metallopeptidase inhibitor 2; Complexes with metalloproteinases (such as collagenases) and irreversibly inactivates them. Known to act on MMP - 1, MMP - 2, MMP - 3, MMP - 7, MMP - 8, MMP - 9, MMP - 10, MMP - 13, MMP - 14, MMP - 15, MMP - 16 and MMP - 19 (220 aa)
22. NOTCH3 Notch homolog 3 (Drosophila); Functions as a receptor for membrane - bound ligands Jagged1, Jagged2 and Delta1 to regulate cell - fate determination. Upon ligand activation through the released notch intracellular domain (NICD) it forms a transcriptional activator complex with RBP- J kappa and activates genes of the enhancer of split locus. Affects the implementation of differentiation, proliferation and apoptotic programs (2321 aa)
23. C9 complement component 9; Constituent of the membrane attack complex (MAC) that plays a key role in the innate and adaptive immune response by forming pores in the plasma membrane of target cells. C9 is the pore - forming subunit of the MAC (559 aa)
24. TF transferrin; Transferrins are iron binding transport proteins which can bind two Fe(3+) ions in association with the binding of an anion, usually bicarbonate. It is responsible for the transport of iron from sites of absorption and heme degradation to those of storage and utilization. Serum transferrin may also have a further role in stimulating cell proliferation (698 aa)
25. VDAC1 voltage - dependent anion channel 1 pseudogene 1; Forms a channel through the mitochondrial outer membrane and also the plasma membrane. The channel at the outer mitochondrial membrane allows diffusion of small hydrophilic molecules; in the plasma membrane it is involved in cell volume regulation and apoptosis. It adopts an open conformation at low or zero membrane potential and a closed conformation at potentials above 30 - 40 mV. The open state has a weak anion selectivity whereas the closed state is cation selective. May participate in the formation of the permeability transition pore (283 aa)
26. PRDX5 peroxiredoxin 5; Reduces hydrogen peroxide and alkyl hydroperoxides with reducing equivalents provided through the thioredoxin system. Involved in intracellular redox signaling (214 aa)
27. TIMP3 TIMP metallopeptidase inhibitor 3; Complexes with metalloproteinases (such as collagenases) and irreversibly inactivates them. May form part of a tissue - specific acute response to remodeling stimuli. Known to act on MMP - 1, MMP - 2, MMP - 3, MMP - 7, MMP - 9, MMP - 13, MMP - 14 and MMP - 15 (211 aa)
28. TTLL8 tubulin tyrosine ligase - like family, member 8; Monoglycylase which modifies both tubulin and non - tubulin proteins, generating side chains of glycine on the gamma - carboxyl groups of specific glutamate residues of target proteins. Mono-

International Journal of Scientific & Engineering Research, Volume 8, Issue 2, February -2017
ISSN 2229-5518

glycylates tubulin, with a preference for alpha - tubulin toward beta - tubulin. Has the ability to modify non -tubulin proteins such as ANP32A, ANP32B, SET and NCL. Involved in the side - chain initiation step of the glycylation reaction by adding a single glycine chain to generate monoglycine side chains. Not involved in elongation step of the polyglycylation (834 aa)

29. RLBP1 retinaldehyde binding protein 1; Carries 11 - cis - retinol and 11 - cis - retinaldehyde as endogenous ligands and may be a functional component of the visual cycle (317 aa)
30. SERPING1 serpin peptidase inhibitor, clade G (C1 inhibitor), member 1; Activation of the C1 complex is under control of the C1 - inhibitor. It forms a proteolytically inactive stoichiometric complex with the C1r or C1s proteases. May play a potentially crucial role in regulating important physiological pathways including complement activation, blood coagulation, fibrinolysis and the generation of kinins. Very efficient inhibitor of FXIIa. Inhibits chymotrypsin and kallikrein (500 aa)
31. XPC xeroderma pigmentosum, complementation group C; Involved in DNA excision repair. May play a part in DNA damage recognition and/or in altering chromatin structure to allow access by damage - processing enzymes (940 aa)
32. ATP5O ATP synthase, H+ transporting, mitochondrial F1 complex, O subunit; Mitochondrial membrane ATP synthase (F(1)F(0) ATP synthase or Complex V) produces ATP from ADP in the presence of a proton gradient across the membrane which is generated by electron transport complexes of the respiratory chain. F -type ATPases consist of two structural domains, F(1) - containing the extramembraneous catalytic core and F(0) - containing the membrane proton channel, linked together by a central stalk and a peripheral stalk. (213 aa)
33. CRYAA crystallin, alpha A; May contribute to the transparency and refractive index of the lens (173 aa)
34. CRYBA2 crystallin, beta A2; Crystallins are the dominant structural components of the vertebrate eye lens (197 aa)
35. ALB albumin; Serum albumin, the main protein of plasma, has a good binding capacity for water, Ca(2+), Na (+), K(+), fatty acids, hormones, bilirubin and drugs. Its main function is the regulation of the colloidal osmotic pressure of blood (609 aa)
36. CRABP1 cellular retinoic acid binding protein 1; Cytosolic CRABPs may regulate the access of retinoic acid to the nuclear retinoic acid receptors (137 aa)
37. PHB prohibitin; Prohibitin inhibits DNA synthesis. It has a role in regulating proliferation. As yet it is unclear if the protein or the mRNA exhibits this effect. May play a role in regulating mitochondrial respiration activity and in aging (272 aa)
38. PRDX2 peroxiredoxin 2; Involved in redox regulation of the cell. Reduces peroxides with reducing equivalents provided through the thioredoxin system. It is not able to receive electrons from glutaredoxin. May play an important role in eliminating peroxides generated during metabolism. Might participate in the signaling cascades of growth factors and tumor necrosis factor- alpha by regulating the intracellular concentrations of H(2)O(2) (198 aa)
39. BCL2L1 BCL2 - like 1; Potent inhibitor of cell death. Isoform Bcl - X(L) anti - apoptotic activity is inhibited by association with SIVA isoform 1. Inhibits activation of caspases (By similarity). Appears to regulate cell death by blocking the voltage - dependent anion channnel (VDAC) by binding to it and preventing the release of the caspase activator, cytochrome c, from the mitochondrial membrane. The Bcl - X(S) isoform promotes apoptosis (233 aa)
40. HSPA4 heat shock 70kDa protein 4 (840 aa) EEF2 eukaryotic translation elongation factor 2; This protein promotes the GTP-dependent translocation of the nascent protein chain from the A- site to the P - site of the ribosome (858 aa)
41. ATP5S ATP synthase, H+ transporting, mitochondrial F0 complex, subunit s (factor B); Involved in regulation of mitochondrial membrane ATP synthase. Necessary for H(+) conduction of ATP synthase (215 aa)
42. PLG plasminogen; Plasmin dissolves the fibrin of blood clots and acts as a proteolytic factor in a variety of other processes including embryonic development, tissue remodeling, tumor invasion, and inflammation; in ovulation it weakens the walls of the Graafian follicle. It activates the urokinase -type plasminogen activator, collagenases and several complement zymogens, such as C1 and C5. It cleaves fibrin, fibronectin, thrombospondin, laminin and von Willebrand factor. Its role in tissue remodeling and tumor invasion may be modulated by CSPG4 (810 aa)
43. ENSG00000173213 Tubulin beta - 8 chain B ; Tubulin is the major constituent of microtubules. It binds two moles of GTP, one at an exchangeable site on the beta chain and one at a non - exchangeable site on the alpha - chain (By similarity) (444 aa)
44. DPYSL2 dihydropyrimidinase - like 2; Necessary for signaling by class 3 semaphorins and subsequent remodeling of the cytoskeleton. Plays a role in axon guidance, neuronal growth cone collapse and cell migration (By similarity) (572 aa)
45. CRYGS crystallin, gamma S; Crystallins are the dominant structural components of the vertebrate eye lens (178 aa)
46. CLU clusterin; Not yet clear. It is known to be expressed in a variety of tissues and it seems to be able to bind to cells, membranes and hydrophobic proteins. It has been associated with programmed cell death (apoptosis) (501 aa)
47. SWAP70 SWAP switching B - cell complex 70kDa subunit; Phosphatidylinositol 3,4,5 -trisphosphate - dependent guanine nucleotide exchange factor (GEF) which, independently of RAS, transduces signals from tyrosine kinase receptors to RAC. It also mediates signaling of membrane ruffling. Regulates the actin cytoskeleton as an effector or adapter protein in response to agonist stimulated phosphatidylinositol (3,4) - bisphosphate production and cell protrusion (585 aa)
48. PKM2 pyruvate kinase, muscle; Glycolytic enzyme that catalyzes the transfer of a phosphoryl group from phosphoenolpyruvate (PEP) to ADP, generating ATP. Stimulates POU5F1 - mediated transcriptional activation. Plays a general role in caspase independent cell death of tumor cells. The ratio betwween the highly active tetrameric form and nearly inactive dimeric form determines whether glucose carbons are channeled to biosynthetic processes or used for glycolytic ATP production. The transition between the 2 forms contributes to the control of glycolysis and is important for tumor cell proliferation (531 aa)
49. FES feline sarcoma oncogene (822 aa) RGS19 regulator of G - protein signaling 19; Inhibits signal transduction by increasing the GTPase activity of G protein alpha subunits thereby driving them into their inactive GDP - bound form. Binds to G - alpha subfamily 1 members, with the order G(i)a3 > G(i)a1 > G(o)a >> G(z)a/G(i)a2. Activity on G(z) - alpha is inhibited by phosphorylation and palmitoylation of the G - protein (217 aa)
50. HIF1A hypoxia inducible factor 1, alpha subunit (basic helix - loop - helix transcription factor); Functions as a master transcriptional regulator of the adaptive response to hypoxia. Under hypoxic conditions activates the transcription of over 40 genes, including, erythropoietin, glucose transporters, glycolytic en-

International Journal of Scientific & Engineering Research, Volume 8, Issue 2, February -2017
ISSN 2229-5518

zymes, vascular endothelial growth factor, and other genes whose protein products increase oxygen delivery or facilitate metabolic adaptation to hypoxia. Plays an essential role in embryonic vascularization, tumor angiogenesis and pathophysiology of ischemic disease. Binds to core DNA (826 aa)

51. WDR64 WD repeat domain 64 (634 aa)
52. PRDX6 peroxiredoxin 6; Involved in redox regulation of the cell. Can reduce H(2)O(2) and short chain organic, fatty acid, and phospholipid hydroperoxides. May play a role in the regulation of phospholipid turnover as well as in protection against oxidative injury (224 aa)
53. SPANXC SPANX family, member C (97 aa) RGR retinal G protein coupled receptor; Receptor for all - trans - and 11 - cis - retinal. Binds preferentially to the former and may catalyze the isomerization of the chromophore by a retinochrome - like mechanism (295 aa)
54. CFH complement factor H; Factor H functions as a cofactor in the inactivation of C3b by factor I and also increases the rate of dissociation of the C3bBb complex (C3 convertase) and the (C3b)NBB complex (C5 convertase) in the alternative complement pathway (1231 aa)
55. LMNA lamin A/C; Lamins are components of the nuclear lamina, a fibrous layer on the nucleoplasmic side of the inner nuclear membrane, which is thought to provide a framework for the nuclear envelope and may also interact with chromatin. Lamin A and C are present in equal amounts in the lamina of mammals (664 aa)
56. PMVK phosphomevalonate kinase (192 aa) BUB3 budding uninhibited by benzimidazoles 3 homolog (yeast); Required for kinetochore localization of BUB1 (328 aa)
57. PGAM1 phosphoglycerate mutase 1 (brain); Interconversion of 3 - and 2 - phosphoglycerate with 2,3 bisphosphoglycerate as the primer of the reaction. Can also catalyze the reaction of EC 5.4.2.4 (synthase) and EC 3.1.3.13 (phosphatase), but with a reduced activity (254 aa)
58. VDAC2 voltage - dependent anion channel 2; Forms a channel through the mitochondrial outer membrane that allows diffusion of small hydrophilic molecules. The channel adopts an open conformation at low or zero membrane potential and a closed conformation at potentials above 30 - 40 mV. The open state has a weak anion selectivity whereas the closed state is cation - selective (294 aa)
59. PPA1 pyrophosphatase (inorganic) 1 (289 aa) DES desmin; Desmin are class - III intermediate filaments found in muscle cells. In adult striated muscle they form a fibrous network connecting myofibrils to each other and to the plasma membrane from the periphery of the Z - line structures (470 aa)
60. TXN thioredoxin; Participates in various redox reactions through the reversible oxidation of its active center dithiol to a disulfide and catalyzes dithiol - disulfide exchange reactions. Plays a role in the reversible S nitrosylation of cysteine residues in target proteins, and thereby contributes to the response to intracellular nitric oxide. Nitrosylates the active site Cys of CASP3 in response to nitric oxide (NO), and thereby inhibits caspase - 3 activity (105 aa)
61. COL5A2 collagen, type V, alpha 2; Type V collagen is a member of group I collagen (fibrillar forming collagen). It is a minor connective tissue component of nearly ubiquitous distribution. Type V collagen binds to DNA, heparan sulfate, thrombospondin, heparin, and insulin. Type V collagen is a key determinant in the assembly of tissue - specific matrices (1499 aa)
62. CKAP4 cytoskeleton - associated protein 4 (602 aa)
63. GSTK1 glutathione S -transferase kappa 1; Significant glutathione conjugating activity is found only with the model substrate, 1 - chloro - 2,4 - dinitrobenzene (CDNB) (282 aa)
64. HSP90AA4P Putative heat shock protein HSP 90 - beta - 3 (Heat shock protein 90 - beta c)(Heat shock protein 90Bc); Molecular chaperone (597 aa)
65. CASP5 caspase 5, apoptosis - related cysteine peptidase; Mediator of programmed cell death (apoptosis) (447 aa)
66. TPI1 triosephosphate isomerase 1 (249 aa)
67. NSF N - ethylmaleimide - sensitive factor; Required for vesicle - mediated transport. Catalyzes the fusion of transport vesicles within the Golgi cisternae. Is also required for transport from the endoplasmic reticulum to the Golgi stack. Seem to function as a fusion protein required for the delivery of cargo proteins to all compartments of the Golgi stack independent of vesicle origin (744 aa)
68. TBC1D14 TBC1 domain family, member 14; May act as a GTPase - activating protein for Rab family protein(s) (By similarity) (693 aa)
69. IMMT inner membrane protein, mitochondrial (mitofilin) (758 aa) CFB complement factor B (621 aa)
70. VDAC3 voltage - dependent anion channel 3; Forms a channel through the mitochondrial outer membrane that allows diffusion of small hydrophilic molecules (284 aa)
71. EEF1D eukaryotic translation elongation factor 1 delta (guanine nucleotide exchange protein); EF- 1 - beta and EF - 1 delta stimulate the exchange of GDP bound to EF - 1 - alpha to GTP (647 aa)
72. GDI1 GDP dissociation inhibitor 1; Regulates the GDP/GTP exchange reaction of most Rab proteins by inhibiting the dissociation of GDP from them, and the subsequent binding of GTP to them (447 aa)
73. ENSG00000224156 Tubulin beta chain (Tubulin beta - 5 chain); Tubulin is the major constituent of microtubules. It binds two moles of GTP, one at an exchangeable site on the beta chain and one at a non - exchangeable site on the alpha - chain (444 aa)
74. TXNRD1 thioredoxin reductase 1; Isoform 1 may possess glutaredoxin activity as well as thioredoxin reductase activity and induces actin and tubulin polymerization, leading to formation of cell membrane protrusions. Isoform 4 enhances the transcriptional activity of estrogen receptors alpha and beta while isoform 5 enhances the transcriptional activity of the beta receptor only. Isoform 5 also mediates cell death induced by a combination of interferon - beta and retinoic acid (651 aa)
75. BUB1B budding uninhibited by benzimidazoles 1 homolog beta (yeast) (1050 aa)
76. BCL2L11 BCL2 - like 11 (apoptosis facilitator); Induces apoptosis. (198 aa)
77. VHL von Hippel - Lindau tumor suppressor; Involved in the ubiquitination and subsequent proteasomal degradation (213 aa)
78. EGLN1 egl nine homolog 1 (C. elegans); Catalyzes the post-translational formation of 4 - hydroxyproline (426 aa)
79. TFRC transferrin receptor (p90, CD71); Cellular uptake of iron occurs via receptor- mediated endocytosis (760 aa)
80. HIF1AN hypoxia inducible factor 1, alpha subunit inhibitor; Hydroxylates HIF- 1 alpha at 'Asp - 803 (349 aa)
81. PLAU plasminogen activator, urokinase; Specifically cleave the zymogen plasminogen to form the activ [...] (431 aa)
82. COL5A1 collagen, type V, alpha 1; Type V collagen is a member of group I collagen (fibrillar forming) (1838 aa)

International Journal of Scientific & Engineering Research, Volume 8, Issue 2, February -2017
ISSN 2229-5518

83. MAP3K5 mitogen - activated protein kinase kinase kinase 5; Component of a protein kinase signal transduction (1374 aa)
84. RAD23B RAD23 homolog B (S. cerevisiae); Plays a central role both in proteosomal degradation of misfolded proteins (409 aa)

Acknowledgments

We thank Dr. Harold J. Sheedlo (University of North Texas Health Science Center) for providing HRP cells. We thank Dr. Ruonan Zhang, Hyunju Lee, Alex Keim, Thagriki Dluya, and Dr. Hilal Arnouk for their excellent technical assistance. This study was supported by the Century II Equipment Fund, Research Excellence Fund from Michigan Technological University, Equipment Fund from NSF, Research and Teaching Assistantship from American University of Nigeria. This work was supported in part by an unrestricted grant from Research to Prevent Blindness to the University of Utah Department of Ophthalmology and Visual Sciences. The authors thank Dr. Jonah Samuel for his critical reading and suggestions.

S.S., O.S., J.Y.U., W.H., F.L., M.N. performed biochemical experiments and analyzed bioinformatics data. P.S., M.B., D.W.C., D.R.G. and W.J.J. supervised experiments and discussed the results. W.J.J. designed the study and all authors wrote the paper.

REFERENCES

[1] A. Paradela, J.P. Albar, Advances in the analysis of protein phosphorylation., J. Proteome Res. 7 (2008) 1809–18. doi:10.1021/pr7006544.

[2] O. Strauss, The retinal pigment epithelium in visual function., Physiol. Rev. 85 (2005) 845–81. doi:10.1152/physrev.00021.2004.

[3] C.L. Nordgaard, P.P. Karunadharma, X. Feng, T.W. Olsen, D. a Ferrington, Mitochondrial proteomics of the retinal pigment epithelium at progressive stages of age-related macular degeneration., Invest. Ophthalmol. Vis. Sci. 49 (2008) 2848–55. doi:10.1167/iovs.07-1352.

[4] C.L. Nordgaard, K.M. Berg, R.J. Kapphahn, C. Reilly, X. Feng, T.W. Olsen, D. a Ferrington, Proteomics of the retinal pigment epithelium reveals altered protein expression at progressive stages of age-related macular degeneration., Invest. Ophthalmol. Vis. Sci. 47 (2006) 815–22. doi:10.1167/iovs.05-0976.

[5] M.R. Terluk, R.J. Kapphahn, L.M. Soukup, H. Gong, C. Gallardo, S.R. Montezuma, D. a Ferrington, Investigating mitochondria as a target for treating age-related macular degeneration., J. Neurosci. 35 (2015) 7304–11. doi:10.1523/JNEUROSCI.0190-15.2015.

[6] M. a Zarbin, Current concepts in the pathogenesis of age-related macular degeneration., Arch. Ophthalmol. 122 (2004) 598–614. doi:10.1001/archopht.122.4.598.

[7] H. Lee, H. Chung, H. Arnouk, F. Lamoke, R.C. Hunt, W.J.M. Hrushesky, P. a Wood, S.H. Lee, W.J. Jahng, Cleavage of the retinal pigment epithelium-specific protein RPE65 under oxidative stress., Int. J. Biol. Macromol. 47 (2010) 104–8. doi:10.1016/j.ijbiomac.2010.05.014.

[8] R. Zhang, W.J.M. Hrushesky, P. a Wood, S.H. Lee, R.C. Hunt, W.J. Jahng, Melatonin reprogrammes proteomic profile in light-exposed retina in vivo., Int. J. Biol. Macromol. 47 (2010) 255–60. doi:10.1016/j.ijbiomac.2010.04.013.

[9] S.R. Sripathi, W. He, O. Sylvester, M. Neksumi, J.-Y. Um, T. Dluya, P.S. Bernstein, W.J. Jahng, Altered Cytoskeleton as a Mitochondrial Decay Signature in the Retinal Pigment Epithelium, Protein J. 35 (2016) 179–192. doi:10.1007/s10930-016-9659-9.

[10] A. Lakkaraju, S.C. Finnemann, E. Rodriguez-Boulan, The lipofuscin fluorophore A2E perturbs cholesterol metabolism in retinal pigment epithelial cells., Proc. Natl. Acad. Sci. U. S. A. 104 (2007) 11026–31. doi:10.1073/pnas.0702504104.

[11] S. Umeda, M.T. Suzuki, H. Okamoto, F. Ono, A. Mizota, K. Terao, Y. Yoshikawa, Y. Tanaka, T. Iwata, Molecular composition of drusen and possible involvement of anti-retinal autoimmunity in two different forms of macular degeneration in cynomolgus monkey (Macaca fascicularis)., FASEB J. 19 (2005) 1683–5. doi:10.1096/fj.04-3525fje.

[12] H. Lee, H. Chung, S.H. Lee, W.J. Jahng, Light-induced phosphorylation of crystallins in the retinal pigment epithelium., Int. J. Biol. Macromol. 48 (2011) 194–201. doi:10.1016/j.ijbiomac.2010.11.006.

[13] S.R. Sripathi, O. Sylvester, W. He, T. Moser, J.-Y. Um, F. Lamoke, W. Ramakrishna, P.S. Bernstein, M. Bartoli, W.J. Jahng, Prohibitin as the Molecular Binding Switch in the Retinal Pigment Epithelium, Protein J. 35 (2016) 1–16. doi:10.1007/s10930-015-9641-y.

[14] W.J. Jahng, C. David, N. Nesnas, K. Nakanishi, R.R. Rando, A cleavable affinity biotinylating agent reveals a retinoid binding role for RPE65., Biochemistry. 42 (2003) 6159–68. doi:10.1021/bi034002i.

[15] L. Xue, D.R. Gollapalli, P. Maiti, W.J. Jahng, R.R. Rando, A palmitoylation switch mechanism in the regulation of the visual cycle., Cell. 117 (2004) 761–71. doi:10.1016/j.cell.2004.05.016.

International Journal of Scientific & Engineering Research, Volume 8, Issue 2, February -2017
ISSN 2229-5518

[16] H. Arnouk, H. Lee, R. Zhang, H. Chung, R.C. Hunt, W.J. Jahng, Early biosignature of oxidative stress in the retinal pigment epithelium., J. Proteomics. 74 (2011) 254–61. doi:10.1016/j.jprot.2010.11.004.

[17] T. Wallimann, G. Wegmann, H. Moser, R. Huber, H.M. Eppenberger, High content of creatine kinase in chicken retina: compartmentalized localization of creatine kinase isoenzymes in photoreceptor cells., Proc. Natl. Acad. Sci. U. S. A. 83 (1986) 3816–9. http://www.pubmedcentral.nih.gov/articlerender.fcgi?artid=323614&tool=pmcentrez&rendertype=abstract.

[18] M. Nita, A. Grzybowski, F.J. Ascaso, V. Huerva, Age-related macular degeneration in the aspect of chronic low-grade inflammation (pathophysiological parainflammation)., Mediators Inflamm. 2014 (2014) 930671. doi:10.1155/2014/930671.

[19] H. Chung, H. Lee, F. Lamoke, W.J.M. Hrushesky, P. a Wood, W.J. Jahng, Neuroprotective role of erythropoietin by antiapoptosis in the retina., J. Neurosci. Res. 87 (2009) 2365–74. doi:10.1002/jnr.22046.

[20] S.R. Sripathi, W. He, J. Um, T. Moser, S. Dehnbostel, K. Kindt, J. Goldman, M.C. Frost, W.J. Jahng, Nitric oxide leads to cytoskeletal reorganization in the retinal pigment epithelium under oxidative stress, Adv. Biosci. Biotechnol. 03 (2012) 1167–1178. doi:10.4236/abb.2012.38143.

[21] P. Yang, J.J. Peairs, R. Tano, N. Zhang, J. Tyrell, G.J. Jaffe, Caspase-8-mediated apoptosis in human RPE cells., Invest. Ophthalmol. Vis. Sci. 48 (2007) 3341–9. doi:10.1167/iovs.06-1340.

[22] S. Blackshaw, R.E. Fraioli, T. Furukawa, C.L. Cepko, Comprehensive analysis of photoreceptor gene expression and the identification of candidate retinal disease genes., Cell. 107 (2001) 579–589. doi:S0092-8674(01)00574-8 [pii].

[23] A.M. Newman, N.B. Gallo, L.S. Hancox, N.J. Miller, C.M. Radeke, M. a Maloney, J.B. Cooper, G.S. Hageman, D.H. Anderson, L. V Johnson, M.J. Radeke, Systems-level analysis of age-related macular degeneration reveals global biomarkers and phenotype-specific functional networks, Genome Med. 4 (2012) 16. doi:10.1186/PREACCEPT-1418491035586234.

[24] M.J. Radeke, C.M. Radeke, Y.-H. Shih, J. Hu, D. Bok, L. V. Johnson, P.J. Coffey, Restoration of mesenchymal retinal pigmented epithelial cells by TGFβ pathway inhibitors: implications for age-related macular degeneration, Genome Med. 7 (2015) 58. doi:10.1186/s13073-015-0183-x.

[25] N. V Strunnikova, a Maminishkis, J.J. Barb, F. Wang, C. Zhi, Y. Sergeev, W. Chen, a O. Edwards, D. Stambolian, G. Abecasis, a Swaroop, P.J. Munson, S.S. Miller, Transcriptome analysis and molecular signature of human retinal pigment epithelium., Hum. Mol. Genet. 19 (2010) 2468–86. doi:10.1093/hmg/ddq129.

[26] L. Biasutto, A. Chiechi, R. Couch, L. a. Liotta, V. Espina, Retinal pigment epithelium (RPE) exosomes contain signaling phosphoproteins affected by oxidative stress, Exp. Cell Res. 319 (2013) 2113–2123. doi:10.1016/j.yexcr.2013.05.005.

[27] A.L. Wang, T.J. Lukas, M. Yuan, N. Du, M.O. Tso, A.H. Neufeld, Autophagy and exosomes in the aged retinal pigment epithelium: possible relevance to drusen formation and age-related macular degeneration., PLoS One. 4 (2009) e4160. doi:10.1371/journal.pone.0004160.

[28] H. Lee, H. Arnouk, S. Sripathi, P. Chen, R. Zhang, M. Bartoli, R.C. Hunt, W.J.M. Hrushesky, H. Chung, S.H. Lee, W.J. Jahng, Prohibitin as an oxidative stress biomarker in the eye, Int. J. Biol. Macromol. 47 (2010) 685–690. doi:10.1016/j.ijbiomac.2010.08.018.

[29] H. Lee, H. Chung, H. Arnouk, F. Lamoke, R.C. Hunt, W.J.M. Hrushesky, P.A. Wood, S.H. Lee, W.J. Jahng, Cleavage of the retinal pigment epithelium-specific protein RPE65 under oxidative stress, Int. J. Biol. Macromol. 47 (2010) 104–108. doi:10.1016/j.ijbiomac.2010.05.014.

[30] S.R. Sripathi, W. He, C.L. Atkinson, J.J. Smith, Z. Liu, B.M. Elledge, W.J. Jahng, Mitochondrial-nuclear communication by prohibitin shuttling under oxidative stress., Biochemistry. 50 (2011) 8342–51. doi:10.1021/bi2008933.

[31] R.A. Whipple, E.M. Balzer, E.H. Cho, M.A. Matrone, J.R. Yoon, S.S. Martin, Vimentin Filaments Support Extension of Tubulin-Based Microtentacles in Detached Breast Tumor Cells, 2 (2008) 5678–5688. doi:10.1158/0008-5472.CAN-07-6589.

[32] Z. Dai, J. Yin, H. He, W. Li, C. Hou, X. Qian, N. Mao, L. Pan, Mitochondrial comparative proteomics of human ovarian cancer cells and their platinum-resistant sublines., Proteomics. 10 (2010) 3789–99. doi:10.1002/pmic.200900685.

[33] M. Krüger, I. Kratchmarova, B. Blagoev, Y.-H. Tseng, C.R. Kahn, M. Mann, Dissection of the insulin signaling pathway via quantitative phosphoproteomics., Proc. Natl. Acad. Sci. U. S. A. 105 (2008) 2451–6. doi:10.1073/pnas.0711713105.

International Journal of Scientific & Engineering Research, Volume 8, Issue 2, February -2017
ISSN 2229-5518

[34] S. Song, M.J. Hanson, B.-F. Liu, L.T. Chylack, J.J.-N. Liang, Protein-protein interactions between lens vimentin and alphaB-crystallin using FRET acceptor photobleaching., Mol. Vis. 14 (2008) 1282–7. http://www.pubmedcentral.nih.gov/articlerender.fcgi?artid=2447818&tool=pmcentrez&rendertype=abstract.

[35] R. Kinouchi, M. Takeda, L. Yang, U. Wilhelmsson, A. Lundkvist, M. Pekny, D.F. Chen, Robust neural integration from retinal transplants in mice deficient in GFAP and vimentin., Nat. Neurosci. 6 (2003) 863–8. doi:10.1038/nn1088.

[36] K. A. West, L. Yan, M. Miyagi, J.S. Crabb, a D. Marmorstein, L. Marmorstein, J.W. Crabb, Proteome survey of proliferating and differentiating rat RPE-J cells., Exp. Eye Res. 73 (2001) 479–91. doi:10.1006/exer.2001.1058.

[37] V.L. Bonilha, S.K. Bhattacharya, K. a West, J. Sun, J.W. Crabb, M.E. Rayborn, J.G. Hollyfield, Proteomic characterization of isolated retinal pigment epithelium microvilli., Mol. Cell. Proteomics. 3 (2004) 1119–27. doi:10.1074/mcp.M400106-MCP200.

[38] F. Schutt, B. Ueberle, M. Schnölzer, F.G. Holz, J. Kopitz, Proteome analysis of lipofuscin in human retinal pigment epithelial cells., FEBS Lett. 528 (2002) 217–21. http://www.ncbi.nlm.nih.gov/pubmed/12297308.

[39] C.S. Alge, S. Suppmann, S.G. Priglinger, A.S. Neubauer, C.A. May, S. Hauck, U. Welge-Lussen, M. Ueffing, A. Kampik, Comparative Proteome Analysis of Native Differentiated and Cultured Dedifferentiated Human RPE Cells, Investig. Opthalmology Vis. Sci. 44 (2003) 3629. doi:10.1167/iovs.02-1225.

[40] C.S. Alge, S.M. Hauck, S.G. Priglinger, A. Kampik, M. Ueffing, Differential protein profiling of primary versus immortalized human RPE cells identifies expression patterns associated with cytoskeletal remodeling and cell survival, J. Proteome Res. 5 (2006) 862–878. doi:10.1021/pr050420t.

[41] E. An, X. Lu, J. Flippin, J.M. Devaney, B. Halligan, E.P. Hoffman, E. Hoffman, N. Strunnikova, K. Csaky, Y. Hathout, Secreted proteome profiling in human RPE cell cultures derived from donors with age related macular degeneration and age matched healthy donors., J. Proteome Res. 5 (2006) 2599–610. doi:10.1021/pr060121j.

[42] A. Decanini, P.R. Karunadharma, C.L. Nordgaard, X. Feng, T.W. Olsen, D. a Ferrington, Human retinal pigment epithelium proteome changes in early diabetes., Diabetologia. 51 (2008) 1051–61. doi:10.1007/s00125-008-0991-2.

[43] K.C. Chan, Q.L. Fu, E.S. Hui, K.F. So, E.X. Wu, Evaluation of the retina and optic nerve in a rat model of chronic glaucoma using in vivo manganese-enhanced magnetic resonance imaging, Neuroimage. 40 (2008) 1166–1174. doi:10.1016/j.neuroimage.2008.01.002.

[44] S. Umeda, M.T. Suzuki, H. Okamoto, F. Ono, A. Mizota, K. Terao, Y. Yoshikawa, Y. Tanaka, T. Iwata, Molecular composition of drusen and possible involvement of anti-retinal autoimmunity in two different forms of macular degeneration in cynomolgus monkey (Macaca fascicularis)., FASEB J. 19 (2005) 1683–5. doi:10.1096/fj.04-3525fje.

[45] H. Galganska, A. Karachitos, M. Wojtkowska, O. Stobienia, M. Budzinska, H. Kmita, Communication between mitochondria and nucleus: putative role for VDAC in reduction/oxidation mechanism., Biochim. Biophys. Acta. 1797 (2010) 1276–80. doi:10.1016/j.bbabio.2010.02.004.

[46] P.G. Sreekumar, R. Kannan, M. Kitamura, C. Spee, E. Barron, S.J. Ryan, D.R. Hinton, αB crystallin is apically secreted within exosomes by polarized human retinal pigment epithelium and provides neuroprotection to adjacent cells., PLoS One. 5 (2010) e12578. doi:10.1371/journal.pone.0012578.

[47] C. Grimm, a Wenzel, F. Hafezi, S. Yu, T.M. Redmond, C.E. Remé, Protection of Rpe65-deficient mice identifies rhodopsin as a mediator of light-induced retinal degeneration., Nat. Genet. 25 (2000) 63–6. doi:10.1038/75614.

[48] J.C. Saari, M. Nawrot, B.N. Kennedy, G.G. Garwin, J.B. Hurley, J. Huang, D.E. Possin, J.W. Crabb, Visual cycle impairment in cellular retinaldehyde binding protein (CRALBP) knockout mice results in delayed dark adaptation., Neuron. 29 (2001) 739–48. doi:10.1016/S0896-6273(01)00248-3.

[49] D. Dong, S.E. Ruuska, D.J. Levinthal, N. Noy, Distinct roles for cellular retinoic acid-binding proteins I and II in regulating signaling by retinoic acid., J. Biol. Chem. 274 (1999) 23695–8. http://www.ncbi.nlm.nih.gov/pubmed/10446126.

[50] X. Yuan, X. Gu, J.S. Crabb, X. Yue, K. Shadrach, J.G. Hollyfield, J.W. Crabb, Quantitative proteomics: comparison of the macular Bruch membrane/choroid complex from age-related macular degeneration and normal eyes., Mol. Cell. Proteomics. 9 (2010) 1031–46. doi:10.1074/mcp.M900523-MCP200.

[51] J.M. Crane, L.K. Tamm, Role of cholesterol in the

International Journal of Scientific & Engineering Research, Volume 8, Issue 2, February -2017
ISSN 2229-5518

formation and nature of lipid rafts in planar and spherical model membranes., Biophys. J. 86 (2004) 2965–79. doi:10.1016/S0006-3495(04)74347-7.

[52] S. Tsalouhidou, C. Argyrou, G. Theofilidis, D. Karaoglanidis, E. Orfanidou, M.G. Nikolaidis, a Petridou, V. Mougios, Mitochondrial phospholipids of rat skeletal muscle are less polyunsaturated than whole tissue phospholipids: implications for protection against oxidative stress., J. Anim. Sci. 84 (2006) 2818–25. doi:10.2527/jas.2006-031.

[53] A.A. Spector, M.A. Yorek, Membrane lipid composition and cellular function., J. Lipid Res. 26 (1985) 1015–35. http://www.ncbi.nlm.nih.gov/pubmed/3906008.

[54] H. Sakaguchi, M. Miyagi, R.M. Darrow, J.S. Crabb, J.G. Hollyfield, D.T. Organisciak, J.W. Crabb, Intense light exposure changes the crystallin content in retina, Exp. Eye Res. 76 (2003) 131–133. doi:10.1016/S0014-4835(02)00249-X.

[55] D. Organisciak, R. Darrow, L. Barsalou, C. Rapp, B. McDonald, P. Wong, Light induced and circadian effects on retinal photoreceptor cell crystallins., Photochem. Photobiol. 87 (2011) 151–9. doi:10.1111/j.1751-1097.2010.00844.x.

[56] J.S. Zigler, C. Zhang, R. Grebe, G. Sehrawat, L. Hackler, S. Adhya, S. Hose, D.S. McLeod, I. Bhutto, W. Barbour, G. Parthasarathy, D.J. Zack, Y. Sergeev, G. a Lutty, J.T. Handa, D. Sinha, Mutation in the βA3/A1-crystallin gene impairs phagosome degradation in the retinal pigmented epithelium of the rat., J. Cell Sci. 124 (2011) 523–31. doi:10.1242/jcs.078790.

[57] J. Xi, R. Farjo, S. Yoshida, T.S. Kern, A. Swaroop, U.P. Andley, A comprehensive analysis of the expression of crystallins in mouse retina, (2003).

[58] R.J. Kapphahn, C.M. Ethen, E. a Peters, L. Higgins, D. a Ferrington, Modified alpha A crystallin in the retina: altered expression and truncation with aging., Biochemistry. 42 (2003) 15310–25. doi:10.1021/bi034774e.

[59] Y.H. Kim, M.Y. Choi, Y.S. Kim, J.M. Han, J.H. Lee, C.H. Park, S.S. Kang, W.S. Choi, G.J. Cho, Protein kinase C delta regulates anti-apoptotic alphaB-crystallin in the retina of type 2 diabetes., Neurobiol. Dis. 28 (2007) 293–303. doi:10.1016/j.nbd.2007.07.017.

[60] P.J. Muchowski, M.M. Valdez, J.I. Clark, AlphaB-crystallin selectively targets intermediate filament proteins during thermal stress., Invest. Ophthalmol. Vis. Sci. 40 (1999) 951–8. http://www.ncbi.nlm.nih.gov/pubmed/10102292.

[61] S. Warburton, W.E. Davis, K. Southwick, H. Xin, A.T. Woolley, G.F. Burton, C.D. Thulin, Proteomic and phototoxic characterization of melanolipofuscin: correlation to disease and model for its origin., Mol. Vis. 13 (2007) 318–29. http://www.pubmedcentral.nih.gov/articlerender.fcgi?artid=2642915&tool=pmcentrez&rendertype=abstract.

[62] S. Warburton, K. Southwick, R.M. Hardman, A.M. Secrest, R.K. Grow, H. Xin, A.T. Woolley, G.F. Burton, C.D. Thulin, Examining the proteins of functional retinal lipofuscin using proteomic analysis as a guide for understanding its origin., Mol. Vis. 11 (2005) 1122–34. http://www.ncbi.nlm.nih.gov/pubmed/16379024.

International Journal of Scientific & Engineering Research, Volume 8, Issue 2, February -2017
ISSN 2229-5518